Lithos 390–391 (2021) 106083

Contents lists available at ScienceDirect

Lithos

journal homepage: www.elsevier.com/locate/lithos

Research article

Evidence for widespread mid-Permian magmatic activity related to rifting following the Variscan orogeny (Western Carpathians)

Gabriel Villaseñor [a,b], Elizabeth J. Catlos [a,*], Igor Broska [c], Milan Kohút [c], Ľubomír Hraško [d], Kimberly Aguilera [a], Thomas M. Etzel [a,e], J. Richard Kyle [a], Daniel F. Stockli [a]

[a] Department of Geological Sciences, Jackson School of Geosciences, The University of Texas at Austin, Austin, TX, United States
[b] School of Earth and Atmospheric Sciences, Georgia Institute of Technology, Department of Geophysics, Atlanta, GA, United States
[c] Earth Science Institute of the Slovak Academy of Sciences, Dúbravská cesta 9, 840 05 Bratislava, Slovak Republic
[d] State Geological Institute of Dionýz Štúr, Mlynská dolina 1, 817 04 Bratislava, Slovak Republic
[e] ExxonMobil, Parkway Spring, TX, United States

ARTICLE INFO

Article history:
Received 2 October 2020
Received in revised form 22 February 2021
Accepted 25 February 2021
Available online 5 March 2021

Keywords:
Zircon
Geochronology
Carpathians
Geochemistry
Slovakia
Granite

ABSTRACT

The Gemeric and Veporic Superunits of the Western Carpathians correlate to the Lower and Middle Austroalpine tectonic units (nappes) of the Eastern Alps. The Gemeric Superunit is characterized by small exposures of rare-metal granites, and their ages impact understanding its tectonic history and how this portion of the Carpathians relates to other Permian age granites exposed throughout Europe and the Western Mediterranean. Here we present new Laser Ablation Inductively Coupled Plasma Mass Spectrometry (LA-ICP-MS) and Secondary Ion Mass Spectrometry (SIMS) zircon U–Pb ages from northern (Hnilec) and southern Gemeric granite exposures (Betliar, Elisabeth Mine, Poproč) and one from the Veporic Superunit (Klenovec). Geochemical analyses of Betliar and Klenovec samples indicate they are highly differentiated and fractionated from a clay-rich source, consistent with published reports for these granites. Zircon saturation temperatures average 733 ± 27 °C (Betliar) and 756 ± 61 °C (Klenovec). Most Gemeric granitic zircons are Permian ($n = 231$ spots), with some inherited zircons giving Middle Ordovician to Late Silurian ($n = 26$), and some Triassic ($n = 6$) U–Pb ages. The dominant Permian U–Pb yield crystallization ages of at 264 Ma for the Gemeric granite and 265 Ma for the Veporic Superunit's Klenovec granite (n = 26). Klenovec zircons typically show distinct yellow rims in cathodoluminescence, characteristic of lower temperature overprint (<600 °C). These granite zircon ages overlap those from the radiolarite-bearing metasediments from the Meliata Ocean exposed in the Dobšiná region (263.9 ± 2.7 Ma, LA-ICP-MS, ± 1σ). The detrital zircon U–Pb ages thus imply a possible beginning of sedimentation in the Meliata Ocean as early as the mid-Permian. The genesis of the Gemeric and the Klenovec granites is related to post-collisional extension. These data link the Western Carpathians to a regional widespread occurrence of Permian magmatism in the European Variscan and Western Mediterranean realms, consistent with regional magmatic re-equilibration of the Moho. This scenario likely occurred in response to a thermal surge that involved significant decompression and extension, lower crustal melting, upward displacement of the Moho, and delamination of the mantle-lithosphere that contributed substantially towards Variscan crustal thinning.

1. Introduction

The Gemeric Superunit (or Gemericum) of eastern Slovakia comprises a large portion of the Slovak Ore Mountains (Slovenské Rudohorie; Spiš-Gemer region) located within the Western Carpathians (Fig. 1). The region has been the focus of studies seeking to understand the origin and geochemical evolution of its rare-metal-enriched (Li–Sn–W–Nb–Ta–B–F) S-type granites (Breiter et al., 2015; Broska et al., 2002; Broska and Kubiš, 2019; Kubiš and Broska, 2005) and the relationship of these granites to generating ore deposits, including siderite (Hurai et al., 2008; Jakabská and Rozložník, 1989), siderite±sulfide and stibnite ore (Grecula et al., 1995), magnesite-talc (Hurai et al., 2010; Petrasová et al., 2007; Radvanec et al., 2004), and Sn–W–Mo (Kohút and Stein, 2005).

Besides the presence of its ore-bearing assemblages, the Gemeric Superunit offers important insights into understanding the dynamics of tectonic assembly and reconstruction. Granites that intrude the Gemeric Superunit appear to have distinct petrographic and geochemical characteristics that differ from other Western Carpathian intrusive igneous complexes (e.g., Jakabská and Rozložník, 1989; Petrík and Kohút, 1997; Petrík et al., 2014; Uher and Broska, 1996). It records

* Corresponding author.
E-mail address: ejcatlos@jsg.utexas.edu (E.J. Catlos).

https://doi.org/10.1016/j.lithos.2021.106083

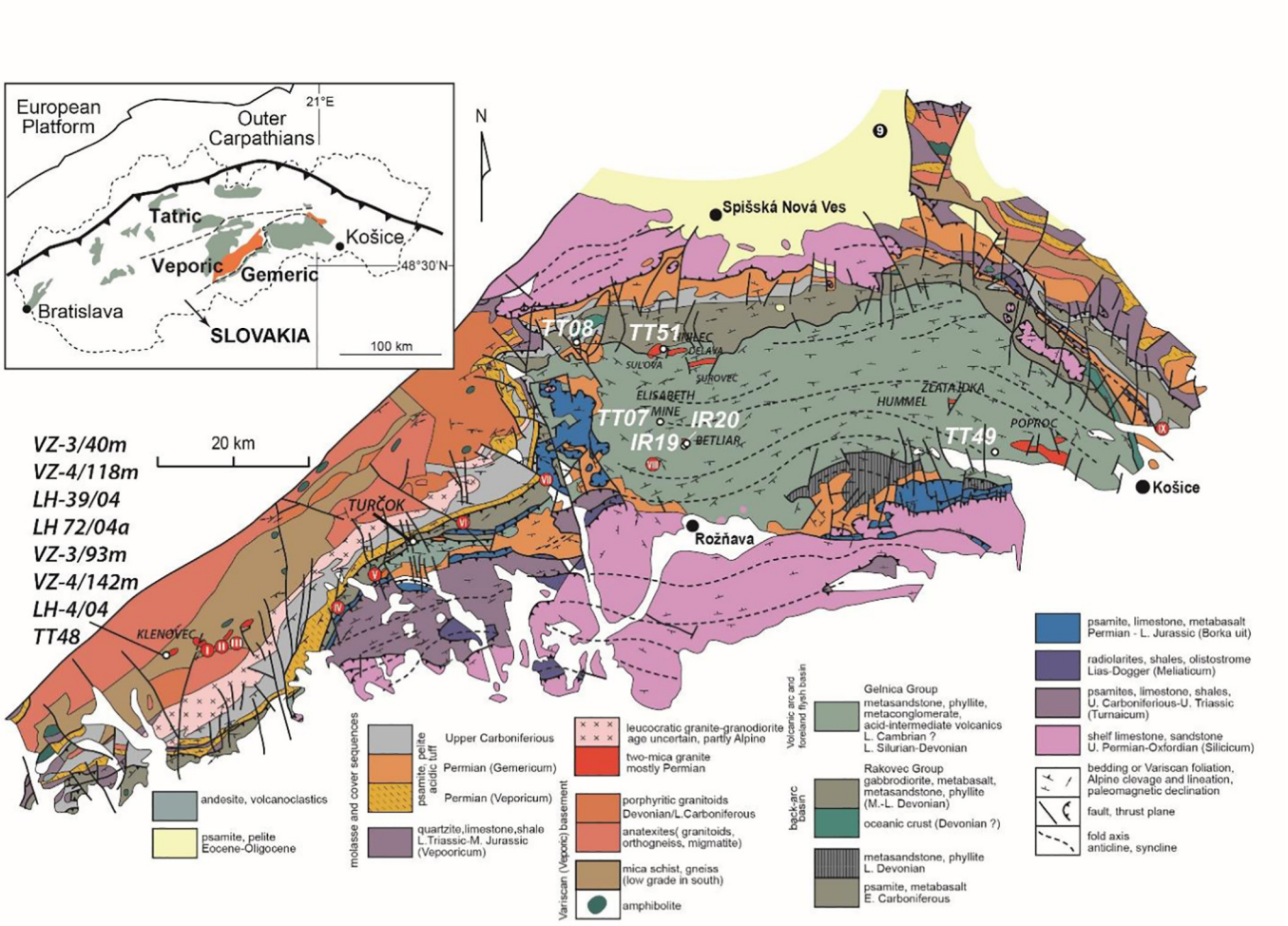

Fig. 1. Geological map of the Gemeric and southern portions of the Veporic superunits showing the locations of samples analyzed in this study. The base map was adapted from Hurai et al. (2010), Lexa et al. (2000), and Lexa et al. (2003). Inset shows the locations of the Variscan basement of the Tatric, Veporic, and Gemeric superunits in Slovakia. Red circles designate other important magnesite-talc deposits: I – Kokava, II – Sinec, III – Samo, IV – Ploské, V – Burda, VI – Jelšava, Ochtiná, VIII – Gemerská Poloma, IX – Košice (Bankov, Medvedia). See Table 3 for sample GPS locations and a summary of their zircon ages.

events associated with Variscan assembly to Permian extension that likewise characterize the Carboniferous-Permian tectonic and magmatic evolutions of central Europe (e.g., Froitzheim et al., 2008; Lexa et al., 2003; Stampfli and Kozur, 2006; Szemerédi et al., 2020).

In this study, we present the results of a campaign to generate zircon U–Pb ages from four granite apophyses that intrude the Gemeric Superunit (Betliar, Hnilec, Poproč, Elisabeth Mine) and one from the underlying Veporic Superunit (Klenovec) (Fig. 1). We also generated whole-rock geochemical data from five distinct magmatic facies of the Betliar granite composite body to relate the results to previous work on the rare-metal granites. We supplement these data with detrital zircon U–Pb data from sedimentary rocks that overlie a fragment of obducted Meliata Ocean crust (Fig. 1). The goal is to use these zircon U–Pb ages to constrain the tectonic evolution of the Gemeric Superunit and relate its importance in broader, regional early Paleozoic and Variscan orogenic events in central and western Europe.

2. Geological background

The Western Carpathians (Fig. 1) consist of three Alpine northward-directed thick-skinned tectonic nappes termed the Tatric, Veporic, and Gemeric Superunits (Froitzheim et al., 2008). These superunits were juxtaposed during the Eo-Alpine (Late Cretaceous) orogeny, although southward-directed thrust-related deformation related to the Variscan orogeny is present in all (Jeřábek et al., 2008; Hrouda and Faryad, 2017). Permian granite intruded both Gemeric and Veporic Superunits during post-collisional extension and initial rifting of the Alpine Tethyan realm (e.g., Poller et al., 2002; Radvanec et al., 2009).

The Gemeric Superunit consists of Paleozoic (Cambrian to Late Carboniferous) meta-sedimentary assemblages, northward-verging thrust imbricates, and partial nappes, the number and terminology of which vary (see Froitzheim et al., 2008; Lexa et al., 2003). It is divided into northern (Klátov, Rakovec, Črmel' and Ochtiná) and southern (Volovec or Gelnica and Štós) segments based on composition and deformation features (Fig. 1) (e.g., Bajaník et al., 1983; Froitzheim et al., 2008; Petrasová et al., 2007; Šefara et al., 2017). The Gemeric granites intrude the Gelnica Group, which belongs to the southern segment, consisting of phyllite and metamorphosed rhyolite and basalt juxtaposed during the Variscan orogeny in the Carboniferous (e.g., Bajaník et al., 1983; Vozárová et al., 2012). In contrast, the northern segment is composed of a series of volcano-sedimentary strata reflecting Paleotethyan subduction and collision affected by polyphase metamorphic events (see

Bajaník et al., 1983; Froitzheim et al., 2008). The Klátov high-grade gneisses and amphibolite comprise the oldest portion of the Gemeric Superunit (ca. 507 Ma, Dallmeyer et al., 1996). The overlying low-grade Rakovec Group consists of metabasalts, phyllites, and black schists with carbonate lenses (e.g., Bajaník et al., 1983; Faryad et al., 2020).

Structurally, the Gemeric Superunit records two generations of thrust deformation (Variscan and Alpine) and two discrete unroofing episodes (Permian and Late Cretaceous) (e.g., Bajaník et al., 1983; Lexa et al., 2003). The Gemeric basement developed a Cretaceous cleavage fan (105–72 Ma; Lexa et al., 2003; Hurai et al., 2008). The asymmetric positive fan structure trends NE-SW and developed transversally across its entire length due to sinistral transpressional deformation along the Transgemeric shear zone (Fig. 1) (Lexa et al., 2003). The structure represents a conjugate intersection of shear surfaces with NW-SE dextral shear zones (e.g., Bajaník et al., 1983; Lexa et al., 2003).

2.1. Background of the granite assemblages

Although the Gemeric granites are only exposed as small apophyses (Fig. 1), they likely link to a continuous 5–8 km-thick post-orogenic intrusive body located at depths of 2–10 km (Šefara et al., 2017). Based on geophysical imaging, this body itself may be a distinct north-verging Alpine nappe, with its upper and lower boundaries dipping southwards (Šefara et al., 2017). The granites are thought to intrude the central portion of the Gelnica Group along deep faults or strike-slip lineaments (Fig. 1) (Finger and Broska, 1999; Hraško et al., 2002; Kohút and Stein, 2005; Petrík et al., 2011; Petrík and Kohút, 1997; Poller et al., 2002; Radvanec et al., 2009; Uher and Broska, 1996). The Betliar, Humel, and Zlatá Idka granites are found in a series of aligned small exposures termed the "southern hotline." The Gul'apalag, a gneiss unit, is also found along the southern hotline. In contrast, the Súľova and Delava granites are associated with the Hnilec Group and are located along a "northern hotline" (Fig. 1) (Radvanec et al., 2009). The age of the granites is thought to young southwards from Hnilec to Zlatá Idka (Radvanec et al., 2009). Table 1 lists published crystallization ages for the granites that range from 290 ± 40 Ma (Rb–Sr Kovach et al., 1986) to 246 ± 5 Ma (U–Pb, Betliar Radvanec et al., 2009). Reported younger Jurassic to Cretaceous ages appear to represent subsequent alteration and metamorphism (e.g., Cambel et al., 1989; Uher and Broska, 1996). This study also provides new insights into the character of the Permian Klenovec granite within the Veporic Superunit, which has a reported Th–Pb monazite age of ~266 Ma and tourmaline mineralization resembling that of the Gemeric granites (Hraško et al., 2002) (Table 1).

Petrographically, several types of Gemeric granites can be distinguished as composite intrusions that were subjected to hydrothermal alteration (Jakabská and Rozložník, 1989; Uher and Broska, 1996). The granites exhibit different mineralogical textures, including coarse-grained, or porphyritic biotite at deeper structural levels, as well as medium-grained muscovite + biotite, and fine-grained greisenized (hydrothermally-altered) two mica in shallower levels (Kohút, 2012; Kubiš and Broska, 2010; Uher and Broska, 1996). In the apexes, rare-metal granites are present (Broska and Kubiš, 2018). The two mica and porphyries show evidence for low-temperature solidi (Ts ~ 600–650 °C), low fO_2, and water and fluorine-rich magma interactions, and emplacement at shallow levels (e.g., 0.5–2.0 kbar, Uher and Broska, 1996).

In geochemical character, the Gemeric granites are high SiO_2, strongly peraluminous, and fractionated with high concentrations of F, B, Rb, Li, Cs, Sn Mo, Be and low concentrations of Sr, Ba, Zr, and V (Broska and Uher, 2001; Kohút, 2012; Petrík and Kohút, 1997; Uher and Broska, 1996). Major minerals include plagioclase, K-feldspar, quartz, muscovite, biotite, and accessory minerals include zircon, apatite, monazite, tourmaline, and garnet (Broska et al., 2002; Uher and Broska, 1996). They are considered a unique type of low temperature (Ts ~ 600–650 °C), tectono-hydrothermal ore-bearing rare metal S-type granites (Sn–F, specialized Ss-type: Breiter et al., 2015; Petrík and Kohút, 1997; Petrík et al., 2014; Uher and Broska, 1996). Their geochemistry points to melt derivation from mature, recycled, sedimentary supracrustal rocks, likely in a collisional setting. Fluids played an essential role in both the development of the granites and the generation of the rare metals found within and associated with them (e.g., Petrík et al., 2014).

Table 1
Previous age obtained from granites in this paper.

Granite name	Age (Ma)	Approach	Reference
Northern hotline Gemeric granite ages			
Hnilec	290 (40)	Rb-Sr	Kovach et al. (1986)
Hnilec type 2	282 (2)	Rb-Sr	Cambel et al. (1989)
Hnilec	276 (13)	Chemical monazite age	Finger and Broska (1999)
Hnilec	263 (0.9)	*Re*-Os molybdenite	Kohút and Stein (2005)
Turčok (A-type)	265–259	U-Pb	Radvanec et al., 2009
Hnilec	250 (18)	U-Pb	Poller et al. (2002)
Sul'ova	257 (4)	U-Pb	Radvanec et al., 2009
Podsúlová (Dhlá Dolina)	151 (14)	Rb-Sr	Kovach et al. (1986)
Podsúlová (Dhlá Dolina)	146 (6)	Rb-Sr	Kovach et al. (1986)
Southern hotline Gemeric Granite ages			
Betliar	277.2 (1.9)	U-Pb	Radvanec et al. (2009)
Zlatá Idka	273 (30)	U-Pb	Poller et al. (2002)
Betliar	272 (47)	Rb-Sr	Kovach et al. (1986)
Humel (surface exposure)	270 (64)	Rb-Sr	Kovach et al. (1986)
Zlatá Idka	251 (16)	Rb-Sr	Kovach et al. (1986)
Betliar	246 (5)	U-Pb	Radvanec et al. (2009)
Humel (deeper portions)	246 (25)	Rb-Sr	Kovach et al. (1986)
Zlatá Idka	223 (32)	Rb-Sr	Kovach et al. (1986)
Zlatá Idka	148 (20)	Rb-Sr	Kovach et al. (1986)
Veporic unit, near Liešnica, Klenovec granite			
Klenovec granite	266 (16)	Th-Pb monazite	Hraško et al. (2002)
Hrončok granite	267 (2)	U-Pb zircon	Ondrejka et al. (2021)

a See Fig. 1 for locations.

The granites themselves may have been derived from crustal sources of Early Paleozoic (Cambrian to Late Carboniferous) remnants that underwent seafloor alteration and were subsequently modified by mineralizing fluids (Kohút, 2012). $^{87}Sr/^{86}Sr$ isotope values (0.711–0.734) also point to derivation from an evolved continental or sedimentary protolith (e.g., Kovach et al. 1986). They were affected by an Alpine deformational and metasomatic overprint during burial below the Meliatic and Silicic nappe system (e.g., Hrouda and Faryad, 2017). In the Gemeric granites alteration assemblages that formed during Late Cretaceous metamorphism consist of albite, phengite, and grossular (e.g., Breiter et al., 2015; Petrík et al., 2011).

Permian A-type granites have also been reported along the northern hotline exposures of the Gemeric unit (e.g., Radvanec et al., 2009; Table 1). We included the location of one such A-type granite (Turčok granite) in the northern portion of the Gemeric unit between the Klenovec and Betliar exposures (Fig. 1).

2.2. Ophiolite exposure, meliata unit

A series of dismembered and incomplete ophiolite slices in the Western Carpathians comprising serpentinites, radiolarian shales and cherts, offer evidence for the presence of the former Meliata Ocean (Fig. 1) (e.g., Faryad et al., 2005; Mock et al., 1998; Plašienka et al., 2019; Putiš et al., 2012). One of these slices is the Meliata Unit, an ophiolite-bearing mélange that forms part of a Jurassic accretionary

flysch complex containing radiolarites, olistostromes, mélanges and ophiolitic bodies (Kozur and Mock, 1997; Mock et al., 1998; see review in Schmid et al., 2008). The Meliata Unit is overall considered a fragment of an ophiolite within an accretionary-subduction wedge that was subsequently obducted onto the Gemeric Superunit (e.g., Putiš et al., 2019). It may correlate with other reported ophiolite packages stretching from the Eastern Alps to the Hellenides (Dallmeyer et al., 2008; Kozur and Mock, 1997; Mock et al., 1998; Schmid et al., 2008), although this remains debated based on timing of obduction (Channell and Kozur, 1997). High-pressure/low-temperature and anchi-grade metamorphism affected the ophiolite and sedimentary strata associated with the Meliata Ocean as well as carbonate platform sediments of the Silica Unit that cover the tectonic nappes and comprise the overall architecture of the Western Carpathians (Faryad et al., 2020 and citations therein).

The opening of the Meliata Ocean during the Permian to early Triassic resulted either from back-arc extension during northwestern-directed subduction of the Paleotethyan Ocean (Froitzheim et al., 2008) (Fig. 9B) or as a result of rifting of the Neotethyan passive continental margin (e.g., Putiš et al., 2019). The Meliata Ocean records back-arc basin (BAB) and normal mid-ocean ridge basalts (N-MORB) (e.g., Faryad et al., 2005; Mock et al., 1998). Sedimentation in the Meliata Ocean continued until the Late Jurassic, after which the radiolarian chert and shale packages experienced metamorphism due to ophiolite obduction (e.g., Putiš et al., 2012). The age of the oldest pelagic sedimentary strata is Middle Triassic (Ladinian) and consists of Middle to Upper Triassic cherty shales (Mock et al., 1998) that contain detrital zircons as young as 243 ± 4 Ma (Putiš et al., 2019). Based on $^{40}Ar/^{39}Ar$ phengitic muscovite ages from blueschists of the Meliata Unit, the closure of the Meliata Ocean occurred during the Late Jurassic (160–150 Ma: Dallmeyer et al., 2008; 155–152 Ma: Faryad and Henjes-Kunst, 1997; 155–140 Ma: Maluski et al., 1993; 170–150 Ma: Putiš et al., 2019). Emplacement and loading of the nappe onto the Central Carpathians occurred in the Early Cretaceous (105.8 ± 1.5 Ma, Dallmeyer et al., 2008; 100 ± 10 Ma, Putiš et al., 2019).

3. Material and methods

3.1. Geochemistry

Overall, eight samples from the Betliar pluton (IR19A-E and IR20A-C) and seven from the Klenovec granite (VZ-3/40 m, VZ-3/93 m, VZ-4/118 m, VZ-4/142 m, LH-39/04, LH 4/04, and LH 72/04) were analyzed for major and trace elements (Fig. 1). We include a Data In Brief article that shows images of several granites and petrographic thin sections, and provides details of the analytical methods (Villaseñor et al., 2021). All Gemeric granite samples consist of quartz + feldspar + albitic plagioclase + biotite ± muscovite ± chlorite ± tourmaline ± fluorite and show evidence of deformation in quartz as undulatory extinction, bulging, and grain-boundary migration. Pinitized (altered) cordierite is present in some samples. The Veporic granite samples are from a small quarry near Klenovec, described by Hraško et al. (2002) with a Permian electron microprobe monazite age (266 ± 16 Ma). The Veporic samples have a similar assemblage as those from the Gemeric Superunit but include Alpine garnet (almandine-grossular) that formed from Fe-rich biotite and muscovite. Chloritized biotite is present in sample TT48. Major and trace element data were collected for Klenovec granite varieties (equigranular, VZ-3/40 m, VZ-4/118 m, LH-39/04; muscovite bearing, LH 72/04a and VZ-3/93 m; fine-grained leucocratic, VZ-4/142 m and LH-4/04). In addition, one sample was analyzed from the northern Gemeric hotline exposure (Hnilec granite, TT51), which was collected from a drill core near Medvedí potok.

Eight samples were collected from the southern hotline Betliar pluton (IR19A-E, and IR20A-C) based on textural appearance. All of the IR19 rocks are from biotite-tourmaline porphyritic portions but differ in how tourmaline appears within the assemblages. Sample IR19A contains disseminated tourmaline, whereas samples IR19B and IR19C contain tourmaline in large cross-cutting veins and nodules. Both IR19C and IR19D contain nodular tourmaline. Samples IR19E and IR20B appear the most intensely deformed and metamorphosed. Sample IR20A contains radiating black tourmaline, whereas IR20C is a dark greisen.

Granite TT07 was collected from the Elisabeth Mine and consists of K-feldspar and plagioclase, as well as biotite, muscovite, quartz, and fluorite. The Elisabeth Mine is a 20-Mt talc deposit that has been mined since 2008 by Euro Talc s.r.*o.* *Major* minerals associated with the deposit are magnesite, dolomite, talc, quartz, and pyrite, and the main talc-forming reaction has been proposed to be metasomatic alteration related to the emplacement of the Elisabeth Mine granite (Petrasová et al., 2007). In this case, the talc-forming reaction is thought to have occurred during the Permian when magnesite + quartz + H_2O = talc + CO_2 formed at conditions of 1 kbar, 430 °C, and XCO_2 of 0.8. Initial magnesite formation may have occurred either during Variscan-related metamorphic events (Radvanec et al., 2004), or during Eo-Alpine nappe stacking, and metamorphism was accompanied by significant hydrothermal alteration (Hurai et al., 2008). Contact zones between the Elisabeth Mine granite and surrounding phyllite were affected by mylonitic Alpine deformation that occurred at lower T (430 °C) but higher P (7 kbar) (Petrasová et al., 2007).

Sample TT49 is from the Poproč pluton located in the eastern portion of the Gemeric Superunit. It was collected from a small quarry next to an abandoned antimony plant. Note that the location and lithology of sample TT49 are similar to that of sample 1 described by Jakabská and Rozložník (1989), sample TT51 similar to their sample 2, and our Betliar samples similar to their sample 3.

3.2. Geochronology

Zircons from granite samples TT51 (Hnilec), IR19A and B, and IR20A and B (Betliar), TT07 (Elisabeth Mine), TT49 (Poproč), and TT48 (Veporic, Klenovec) and sedimentary rock sample TT08 were U–Pb dated using both LA-ICP-MS (University of Texas at Austin) and SIMS (UCLA). Data acquisition parameters are presented in the Data in Brief supplement (Villaseñor et al., 2021) and are summarized in Table 3. Due to the larger uncertainty of the SIMS ages, we resorted to the LA-ICP-MS dating to generate higher-precision results from more zircons grains. LA-ICP-MS ages are reported at the ±2σ level. While the SIMS ages have higher uncertainties, reported at the ±1σ level, the results are consistent with the LA-ICP-MS ages.

We also report detrital zircon U–Pb LA-ICP-MS data from sample TT08, a radiolarite from the Meliata Unit that overlies blueschist and harzburgite-lizardite serpentinite near the city of Dobšiná, Slovakia (Fig. 1). The base of the Meliata Unit in the Dobšiná locality is a highly altered blueschist marble mélange complex (e.g., Mock et al., 1998; Putiš et al., 2019). $^{40}Ar/^{39}Ar$ phengite analyses from the blueschist of the Meliata Unit yield 150-120 Ma (Árkai et al., 2003). Blueschist record metamorphic conditions of 380–460 °C and 9–12 kbar, whereas the overlying ultramafic perovskite-andradite-bearing harzburgite record temperatures of ~350–450 °C (Putiš et al., 2012). The overlying radiolaria-bearing, or pelagic sedimentary strata (including sample TT08) are thought to have been deposited in the Meliata Ocean prior to its closure in the Jurassic (e.g., Putiš et al., 2012). This package dips towards the southeast due to tectonic movements associated with obduction.

We used a FEI Nova Nano SEM Gatan Chroma CL detector to image selected grains. Color CL images are constructed by combining three images of the same area collected using a blue, green, and red filter. Although zircons are often imaged in black and white CL, the use of color allows additional information, including possible chemical changes in trace element contents during the crystallization of zircons. In general, blue-green colors correlate with higher annealing

temperature compared to yellow colors (>800 °C vs. <600 °C, e.g., Tsuchiya et al., 2015).

4. Results

4.1. Geochemistry

We compared the geochemistry of the Betliar and Klenovec samples to those reported from the Gemeric granites elsewhere (Table 2, Figs. 2-4) (Breiter et al., 2015; Kubiš and Broska, 2005, 2010; Petrík et al., 2011; Uher and Broska, 1996). Loss on Ignition values for the Betliar samples range from 0.71 wt% for IR19C to 2.15 wt% for greisenized sample IR20C. Klenovec granite CO_2, H_2O^+, and H_2O^- abundances range from 1.92 wt% (VZ-3/40 m) to 0.45 wt% (LH-72/04), consistent with porphyry-type granites.

Sample IR20C has the highest CaO (0.70 wt%) and Al_2O_3 (14.50 wt%), and the lowest Na_2O (0.13 wt%) and TiO_2 (0.04 wt%) concentrations of all Betliar samples. All Betliar samples have high SiO_2 (from 76.42 wt% in IR19C to 72.91 wt% in IR19A) and low CaO (lowest is only 0.18 wt% in IR19B) concentrations. Samples targeted for geochronology include IR19A, which has the lowest SiO_2 (72.91 wt%) and highest K_2O (5.18 wt%) and Fe_2O_3 (2.22 wt%) and IR20A, which has the highest TiO_2 (0.19 wt%) and lowest Al_2O_3 (12.14 wt%) of all the Betliar samples. Dated sample IR20B has the highest MnO (0.05 wt%), Na_2O (3.56 wt %), and P_2O_5 (0.38 wt%) contents. Klenovec granites also have high SiO_2 (76.33 wt% in sample VA-3/93 m to 70.08 wt in VZ-3/40 m). Fine-grained granite LH-4/04 is unique compared to the other Klenovec samples in that it has the highest CaO concentrations (1.24 wt%); all others contain 0.48 wt% CaO (LH-72/04) to 0.02 wt% (VZ-4/142 m and VZ-3/93 m).

All Betliar and Klenovec granites are strongly peraluminous (Table 2). About half of the Betliar analyses show the granites to be magnesian and calc-alkaline, similar to plutons in the center of large batholiths (Frost et al., 2001). Other samples are calc-alkaline and ferroan two mica granites (IR19C and IR20B). Sample IR19A is alkaline-calcic and ferroan, whereas the greisen sample, IR20C is calcic and magnesian. All Klenovec samples are magnesian, and most are alkali-calcic, consistent with plutons associated with the delamination of overthickened crust (Frost et al., 2001). The zircon saturation temperature of all Betliar samples average 733 ± 27 °C, whereas Klenovec samples average 757 ± 62 °C (Table 2).

Overall, the trace element abundances and ratios from the Betliar and Klenovec samples are consistent with those of *syn*-collisional granites generated from a pelitic source (Fig. 3). These are strongly differentiated and fractionated granites with higher-than-average continental crustal or chondritic values for rare metals and other elements like Be, Ge, Sb, Sn, Ta, W, Y, and Zr (Fig. 3C). In a SiO_2 vs. Zr/Hf plot, some Betliar samples fall within the range of Sn-W-Mo-Be deposits of the greisen type, Li–F granites, but others are barren (Fig. 3D). Fluorine concentrations in the Klenovec samples range from 0.05 wt% (VZ-3/93 m) to 0.15 wt% (VZ-3/40 m). Most granites are enriched in trace elements with respect to chondrite and primitive mantle (Figs. 3E and F). The analyses show significant enrichments with respect to chondrite, except P, Ti, and Eu in the Betliar samples, whereas some analyses of Sr, Eu, and Ti are depleted with respect to the primitive mantle.

Betliar and Klenovec samples also have low REE contents. Betliar sample IR19D has the highest REE content of 224.7 ppm, whereas IR20C has the lowest with only 12.4 ppm. Of the Klenovec samples, LH-39/04 has the highest (161.7 ppm) and VZ-3/93 m (12.23 ppm) the lowest REE contents. Lower Eu contents in these highly evolved rocks are related to Eu fractionation between residual melt and high-temperature fluid interaction (e.g., Irber, 1999). All Betliar and Klenovec analyses show pronounced Eu anomalies (Fig. 4), except for IR20C, which contains <0.05 ppm Eu (below detection limits, Table 2). We explored correlations between the tetrad effect (TE1,3) and K/Rb, Y/Ho, Zr/Hf, Eu/Eu*, Sr/Eu (e.g., Irber, 1999) (Fig. 4). The majority of the previously analyzed Gemeric, Betliar, and Klenovec samples show TE1,3 values / ratios that can be related to increasing degrees of fluid-interactions (e.g., Irber, 1999; Monecke et al., 2002; Zhenhua et al., 1993). Note that this effect may have formed within the magma–fluid system before emplacement or have been inherited from an external fluid influencing the system during or after magma emplacement (Monecke et al., 2002).

4.2. Geochronology

Zircons from the southern Gemeric hotline Betliar (IR19A and B, IR20A and B), Elisabeth mine (TT07), and Poproč (TT49), and one from the northern Gemeric Hnilec body (TT51) granite bodies were U–Pb dated (Fig. 5). We also include data from the Klenovec granite (TT48) in the adjacent Veporic Superunit as a comparison to the Gemeric results. Table 3 summarizes the U–Pb results. Hnilec sample

Table 2
Whole-rock geochemical analysis of samples from the Betliar Pluton.

Gemeric Granite Betliar Pluton								
Analyte Symbol	IR20B	IR19B	IR19C	IR19E	IR20C	IR20A	IR19A	IR 19D
Zircon T_{sat} (°C)[a]	697	709	718	725	730	750	756	781
Fe/Fe+Mg[b]	0.959	0.801	0.946	0.732	0.792	0.816	0.881	0.807
	F	M	F	M	M	M	F	M
MALI[c]	7.36	7.52	7.87	6.99	4.24	7.10	7.88	6.19
	C-A	C-A	C-A	C-A	C	C-A	A-C	C-A
ASI[d]	1.314	1.307	1.170	1.347	2.294	1.249	1.193	1.456

Veporic Granite Klenovec Pluton							
Analyte Symbol	VZ-3/93 m	VZ-4/142 m	LH-4/04	VZ-4/118 m	VZ-3/40 m	LH- 72/04	LH-39/04
Zircon T_{sat} (°C)[a]	653	684	772	791	796	790	810
Fe/Fe+Mg[b]	0.552	0.410	0.754	0.533	0.520	0.767	0.711
	M	M	M	M	M	M	M
MALI[c]	7.46	8.19	6.15	7.40	6.88	6.91	7.83
	C-A	A-C	C-A	A-C	A-C	A-C	A-C
ASI[d]	1.331	1.263	1.257	1.459	1.492	1.374	1.400

[a] See supplementary data for details of the geochemical data. Zircon saturation temperature T_{sat} (°C).
[b] (FeOtotal)/(FeOtotal +MgO). F = ferroan, M = magnesian granites, based on classification in Frost et al. (2001).
[c] MALI = Modified Alkaline Lime Index, C = calcic granite, C-A = calc-alkalic granite, A-C = alkali-calcic granite.
[d] ASI = Aluminosaturation index.

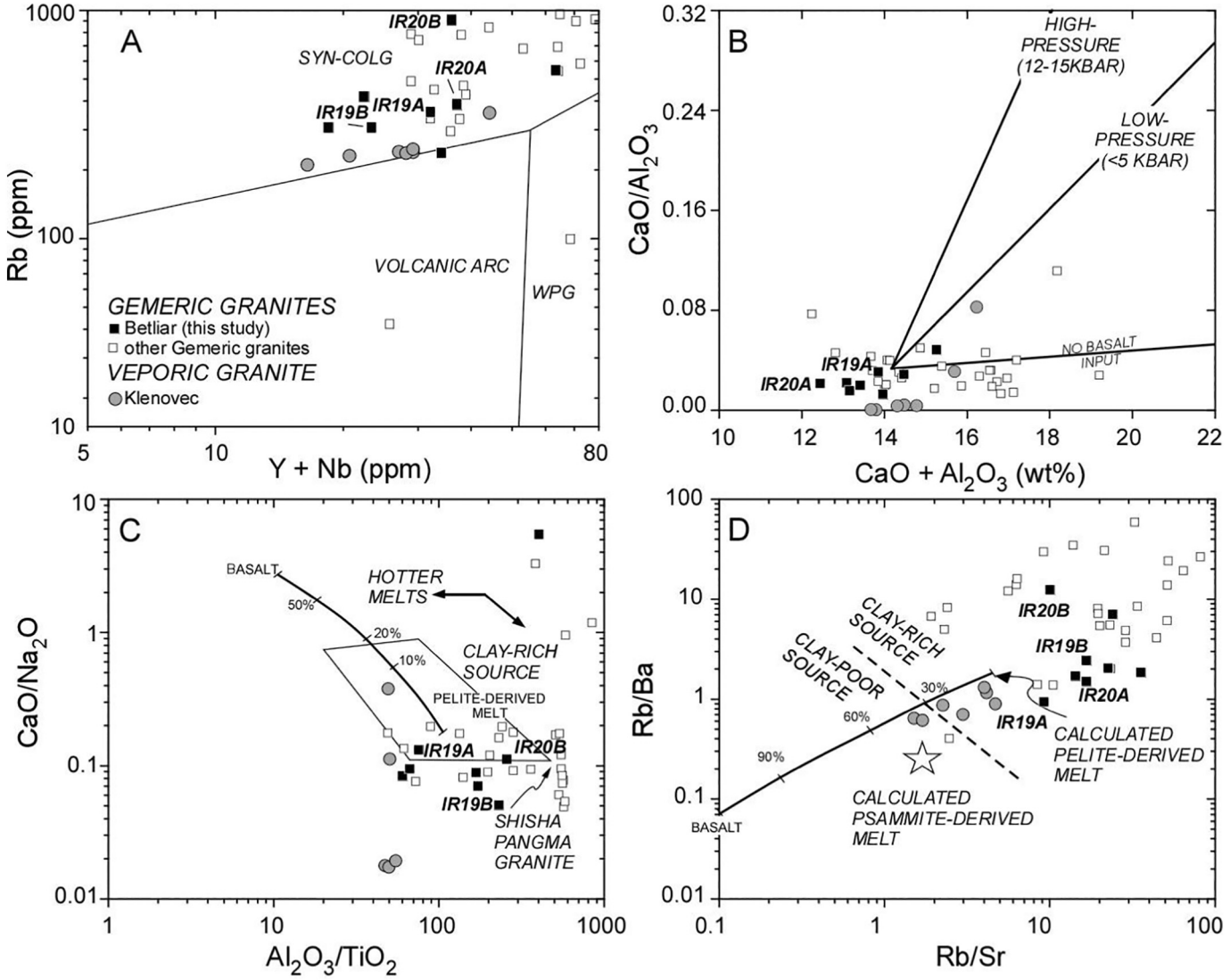

Fig. 2. (A) Y + Nb (ppm) vs. Rb (ppm) discrimination diagram (Pearce et al., 1984) showing Klenovec, Betliar, and other Gemeric granite analyses (Breiter et al., 2015; Kubiš and Broska, 2005; Kubiš and Broska, 2010; Petrík et al., 2011; Uher and Broska, 1996). Syn-collisional (*syn*-colg), volcanic arc, and within plate granite (WPG) fields are labeled. (B) CaO + Al_2O_3 vs. CaO/Al_2O_3 diagram after Patino Douce (1999). Lines indicate trends were high-pressure, low-pressure, and magmas with no basalt input would be located. (C) Al_2O_3/TiO_2 vs. CaO/Na_2O diagram after Sylvester (1998). Quadrilateral outlines field of published data of peraluminous melts from other regions are plotted, and the Shishi Pangma (South Tibet Himalaya) corner is labeled. (D) Rb/Sr vs. Rb/Ba diagram after Sylvester (1998). The dashed line divides clay-rich and clay-poor sources. In panels (C) and (D), a mixing curve between average Phanerozoic basalt and pelite-derived melt is included (see Sylvester, 1998). Percentages of basalt mixing are indicated. Star in panel (D) indicates the location of psammite-derived melt. Betliar samples that were dated (IR19A and B, and IR20A and B) are indicated for reference. See Villaseñor et al. (2021) for the numerical data.

TT51 yielded the most zircons ($n = 42$ grains), whereas samples IR20B and TT49 had the smallest zircon yield (only 11 in Poproč sample TT49 and 12 in Betliar sample IR20B). Villaseñor et al. (2021) show CL images of most of the zircons dated in this paper.

The oldest zircon U–Pb dates are found in Klenovec sample TT48, which yields two discordant Precambrian ages ($^{207}Pb/^{206}Pb$ ages, 2552 ± 18 Ma and 2389 ± 18 Ma, LA-ICP-MS, 27.8% and 26.5% discordant in U–Pb, respectively). These ages are found in the cores of zircons with recrystallized magmatic Permian rims (Fig. 6A and B). Overall, twenty-five spots ($n = 18$ lased spots and 7 SIMS) were placed on ten zircons from sample TT48. Besides the inherited Precambrian ages, SIMS geochronology yields one discordant U–Pb age at 434.7 ± 43.0 Ma (Fig. 6B). All other results are Permian (Table 3). The oldest, most precise Permian age is found in the core of an oscillatory-zoned zircon (272.3 ± 4.3 Ma, LA-ICP-MS, Fig. 6C). This age overlaps within uncertainty of both the oldest and youngest ages obtained using SIMS (285.1 ± 15.0 Ma and 276.2 ± 15.8 Ma, Figs. 6D and E). The youngest, most precise Triassic age from sample TT48 are located on an inner rim (248.6 ± 3.3 Ma, LA-ICP-MS, Fig. 6E). Overall, the zircon U–Pb ages from this granite overlap with those obtained from the Gemeric Superunit (Table 3). Because magmatic assemblages likely do not crystallize over long episodes of geological time, some of the zircons may have experienced Pb loss that is not reflected in Concordia. The only distinct difference we observed between zircons from this sample compared to those from the Gemeric granites was the presence of dull to bright yellow recrystallized zones near zircon rims (identified by arrows in Fig. 6). The yellow color is observed in all zircons we extracted from the Klenovec granite.

Betliar samples IR19A, IR19B, and IR20B, Hnilec sample TT51, and Elisabeth Mine sample TT07 also contain older ages (Table 3; Fig. 7). Eight spots were placed on zircons from the Hnilec granite, which is the northernmost sample collected (Fig. 1), and only 77 of the spots are Permian (Table 3). The oldest inherited zircon in sample TT51 is Cambrian (503 ± 12 Ma, LA-ICP-MS) and is found on a spot near the center of a grain with a Permian-age rim (265.9 ± 3.7 Ma) during laser depth-profiling (Fig. 6F). Three other zircons from the Hnilec

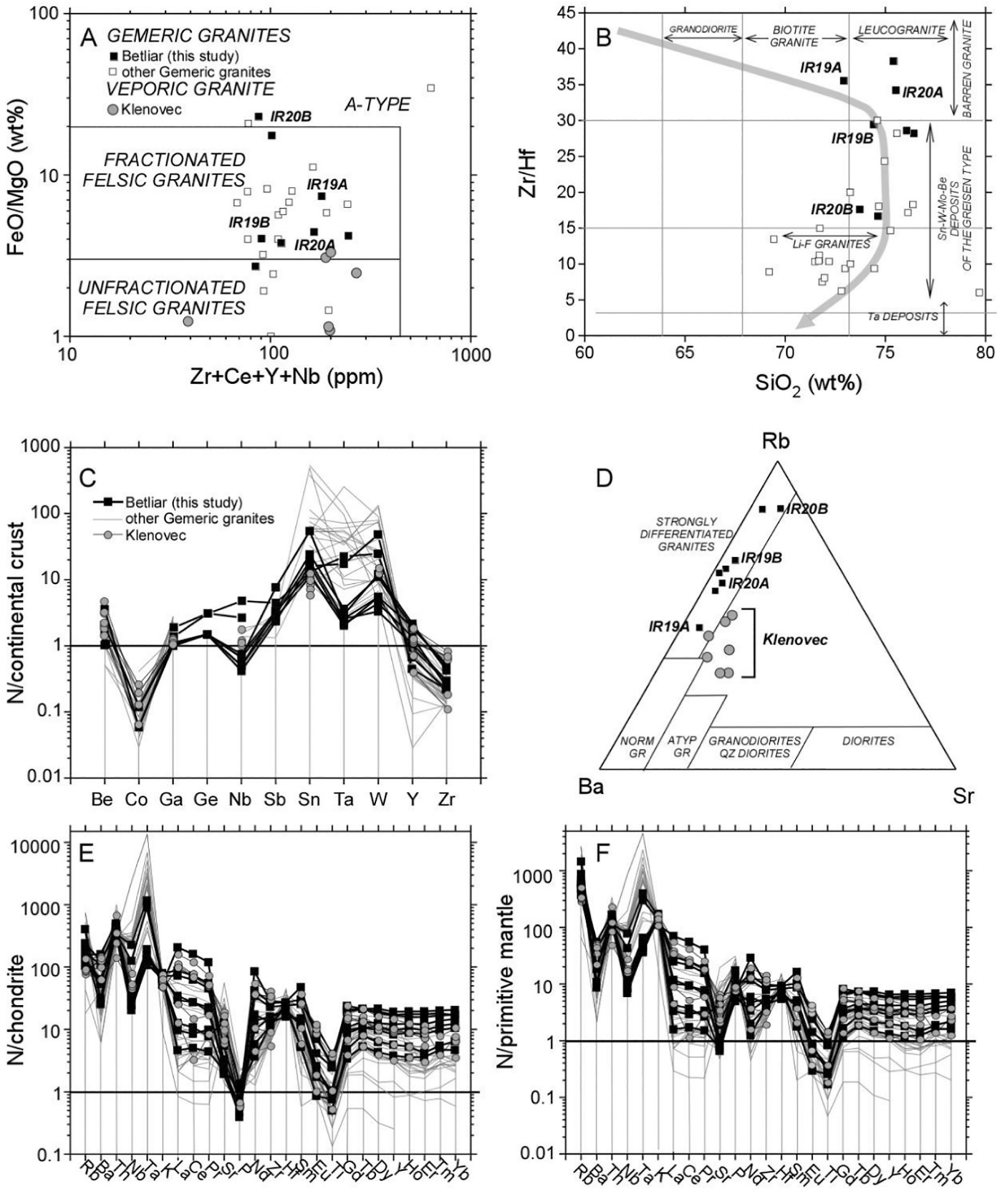

Fig. 3. (A) Zr + Ce + Y + Nb (ppm) vs. FeO/MgO discrimination diagram (Whalen et al., 1987) showing Klenovec, Betliar, and other Gemeric granite samples (Breiter et al., 2015; Kubiš and Broska, 2005; Kubiš and Broska, 2010; Petrík et al., 2011; Uher and Broska, 1996). Fields of A-type granites fractionated and unfractionated are labeled. (B) SiO_2 (wt%) vs. Zr/Hf diagram after Zaraisky et al. (2008). Arrow traces the differentiation trend through the fields of rare-metal granitoids from granodiorite, biotite granite, leucogranite, Li—F granites, and Ta deposits. Sn-W-Mo-Be deposits of the greisen type and barren granite fields are also labeled. (C) Multi-element spider diagram for metal-bearing granites. Elements selected after Dehaine et al. (2019). Y and Zr are normalized to upper continental crust values of Taylor and McLennan (1985), whereas all other elements are normalized to continental crust values of Gao et al. (1998). (D) Rb-Ba-Sr ternary diagram after Horbe et al. (1991). Most Gemeric granites plot in the field of strongly differentiated granites. Also labeled are fields of normal granite (Norm. Gr.), atypical granites (Atyp. Gr.), granodiorite and quartz-diorites, and diorites. Betliar samples that were dated (IR19A and B, and IR20A and B) are indicated for reference. Trace element spider diagram with elements normalized to chondrite (E) and primitive mantle (F) using values in Sun and McDonough (1989). See Villaseñor et al. (2021) for the numerical data.

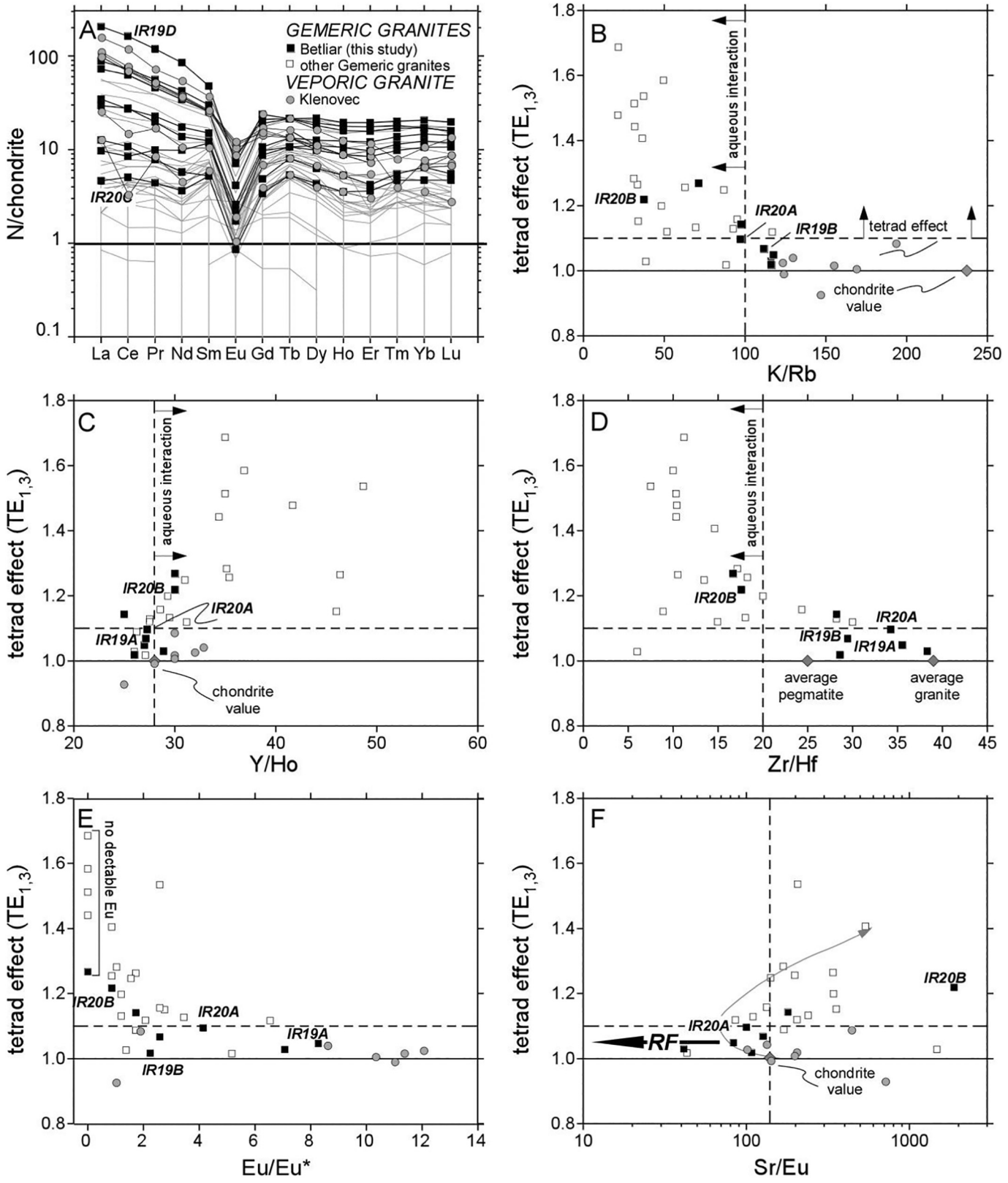

Fig. 4. (A) Chondrite-normalized REE diagram for Betliar and Klenovec (this manuscript) and Gemeric granite samples (see references in other figure captions). Chondrite values from Sun and McDonough (1989). (B) Plot of tetrad effect (TE1,3) vs K/Rb. The horizontal dashed line in this and other panels at TE1,3 values 1.1 and higher indicates that this effect is present in the samples. The K/Rb of chondrite is indicated (235, Sun and McDonough, 1989). K/Rb of <100 is suggested for rocks that have undergone significant degrees of fluid interaction (e.g., Irber, 1999). (C) Plot of TE1,3 vs Y/Ho. The K/Rb of chondrite is indicated (28, Sun and McDonough, 1989). Y/Ho > 28 is suggested for rocks that have undergone significant fluid interaction (e.g., Irber, 1999). (D) Plot of TE1,3 vs. Zr/Hf. Average Zr/Hf values for granite (39) and pegmatite (25) are plotted (Irber, 1999). Zr/Hf > 20 is suggested for rocks that have undergone significant fluid interaction. (E) Plot of TE1,3 vs. Eu/Eu*. Also indicated are samples with Eu contents that are below the detection limit. (F) Plot of TE1,3 vs. Sr/Eu. The K/Rb of chondrite is indicated (125, Sun and McDonough, 1989). The bold arrow shows the direction of Rayleigh fractionation, and the thin arrow follows the trend for Fichtelgebirge granites (Germany) that fractionated to high degrees (Irber, 1999). See Villaseñor et al. (2021) for the numerical data.

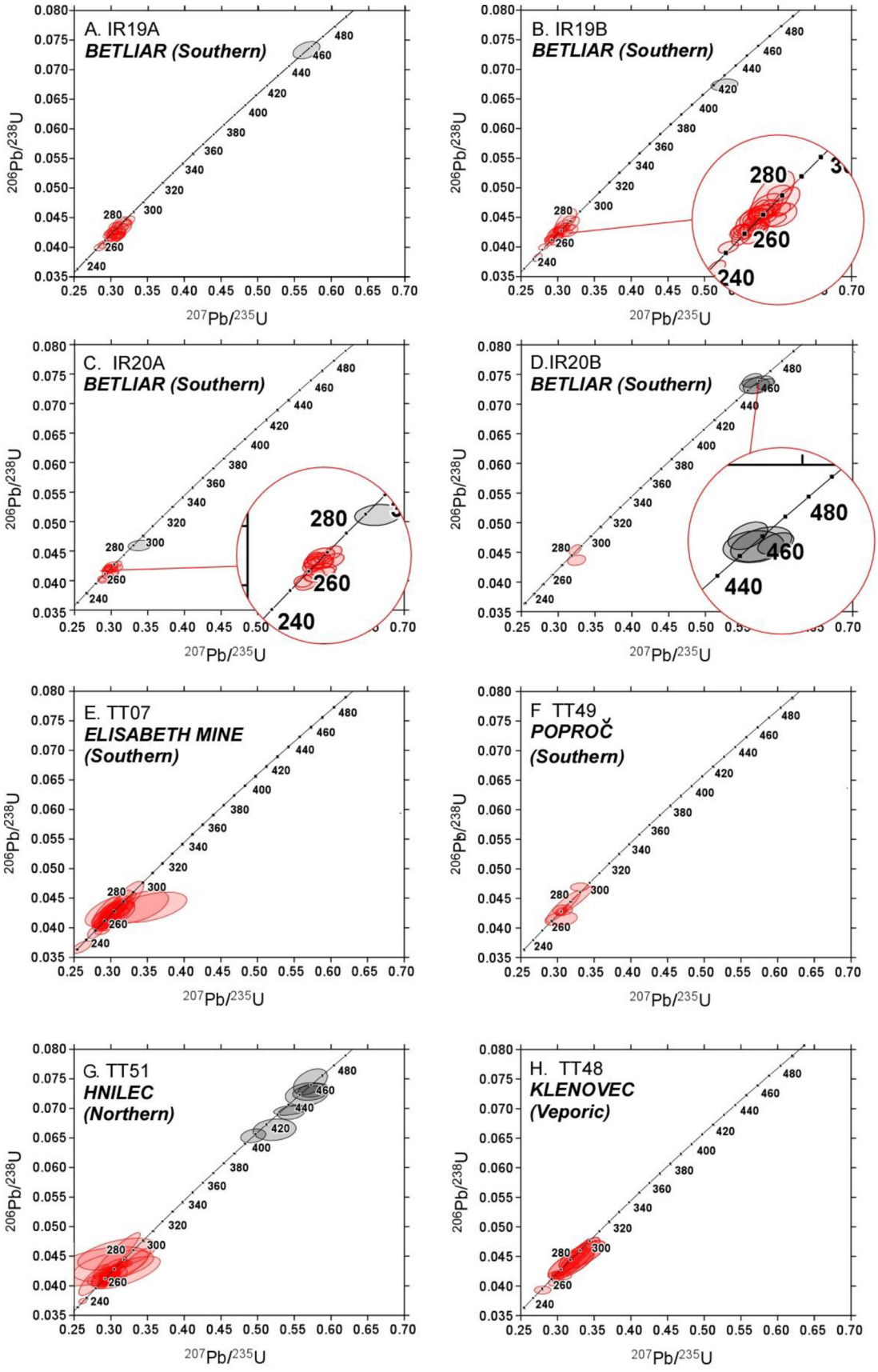

Fig. 5. Concordia diagrams for zircons (filtered for <5% concordance) dated by both LA-ICP-MS and SIMS: (A–D) Betliar pluton, (E) Elisabeth Mine, (F) Poproč, (G) Hnilec, and (H) Klenovec pluton. Permian to Triassic ages are shown in red, older ages shown in gray. See Table 3 for a summary of these results.

Table 3
Summary of zircon ages.a. Sample number with number of spots placed on zircon.
b. Youngest LA-ICP-MS 238U–206Pb age that is <5% concordant.
c. Oldest LA-ICP-MS 238U–206Pb age that is <5% concordant.
d. Youngest concordant zircon 238U–206Pb SIMS age.
e. Oldest concordant zircon 238U–206Pb SIMS age.
f. Average LA-ICP-MS zircon 238U–206Pb age of grains that have Permian or younger absolute ages. Note that most zircon grains from sample IR20B are older than the Permian (average 453.2 ± 5.9 Ma, LA-ICP-MS, so these were not listed in the table.
g. Weighted mean LA-ICP-MS zircon 238U–206Pb age of grains that have Permian or younger absolute ages. Note that most zircon grains from sample IR20B are older than the Permian (weighted mean age of 453.2 ± 6.4 Ma, LA-ICP-MS), so these were not listed in the table.
h. MSWD = Mean Square Weighted Deviation of the LA-ICP-MS ages only.

Sample (n)[a]	Youngest age LA-ICP-MS ^{238}U--^{206}Pb (±2σ) Ma[b]	Oldest age LA-ICP-MS ^{238}U--^{206}Pb (±2σ) Ma[c]	Youngest age SIMS ^{238}U--^{206}Pb (±1σ) Ma[d]	Oldest age SIMS ^{238}U--^{206}Pb (±1σ) Ma[e]	Average ≤ Permian LA-ICP-MS age ^{238}U--^{206}Pb (±2σ) Ma[f]	WM ≤ Permian LA-ICP-MS age ^{238}U--^{206}Pb (±2σ) Ma[g]	MSWD[h]
Northern Gemeric Hnilec TT51 (N 48° 49.549′ E 20° 29.211′)							
TT51 (n = 88)	263.7 (2.2)	463.0 (11.0)	259 (16)	286 (17)	262.9 (3.0)	261.5 (0.1)	7.0
Southern Gemeric Betliar granite IR19 and IR20 (N48°44.16′, E 20°31.74)							
IR19A (n = 44)	252.8 (3.2)	458.4 (7.3)	–	–	268.8 (4.0)	268.2 (0.3)	3.5
IR19B (n = 41)	229.0 (3.6)	420.3 (4.9)	–	–	265.6 (4.3)	264.6 (0.3)	8.7
IR20A (n = 21)	254.0 (3.4)	297.0 (15.0)			265.7 (4.7)	263.5 (0.5)	4.7
IR20B (n = 12)	275.5 (4.4)	286.5 (4.4)			–	–	–
Southern Gemeric Elisabeth Mine TT07 (N 48°45.034′, E 20°29.641′)							
TT07 (n = 46)	232.6 (4.3)	282.1 (7.1)	265 (15)	285 (16)	263.9 (4.0)	263.5 (0.3)	6.1
Southern Gemeric Poproč TT49 (N 48° 43.374′ E 20° 59.004′)							
TT49 (n = 11)	261.9 (6.5)	295.8 (3.4)	275 (16)	284 (14)	273.5 (4.0)	274.1 (1.7)	10.1
Veporic unit, near Liešnica, Klenovec granite TT48 (N 48° 32.760′ E 19° 49.620′)							
TT48 (n = 26)	248.6 (3.3)	272.3 (4.3)	276 (16)	285 (15)	263.1 (3.2)	264.0 (0.7)	3.2

pluton similarly show inherited (older than Permian) cores during laser depth-profiling (463 ± 11 Ma, 414.4 ± 9.1 Ma, and 353.7 ± 3.9 Ma, see Villaseñor et al., 2021 for CL images of these grains).

Inherited zircon of Silurian and Early Devonian age were also found in Betliar sample IR20B (439.2 ± 5.6 Ma and 416.7 ± 7.7 Ma), although other spots on these same grains yielded discordant results. The oldest zircon ages from Elisabeth Mine sample TT07 are imprecise Carboniferous SIMS ages (306 ± 28 Ma, 330 ± 26 Ma), and the same zircons yield more precise Permian LA-ICP-MS results (264.5 ± 2.3 Ma, 267.1 ± 2.5 Ma). While most of the zircons with inherited ages exhibit

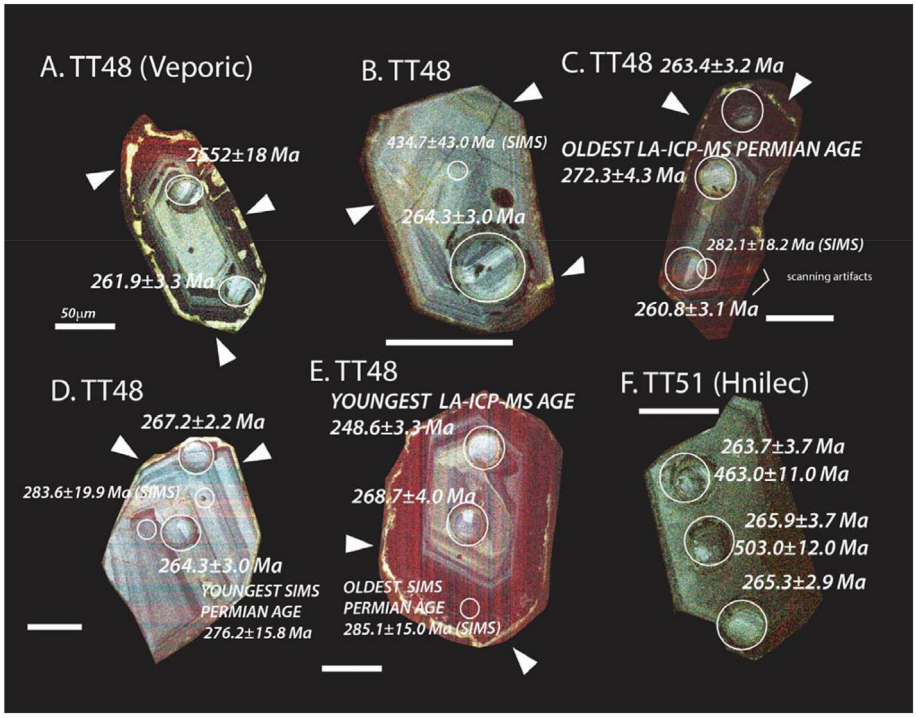

Fig. 6. Color CL images of selected zircons from the Veporic (TT48) and Hnilec granites (TT51). Panels indicate the sample numbers (TT48 and TT51), and the scale bar is 50 μm. All ages have been determined by LA-ICP-MS (±2σ), except when indicated. SIMS ages are ±1σ in smaller font and with a smaller spot diameter. The dated spots are circled in each panel. Arrowheads indicate the locations of brighter yellow CL zones on the rims of zircons from sample TT48, which is a characteristic for this sample. Some of the red lines seen in zircons in panels B and C are an artifact of the scanning process.

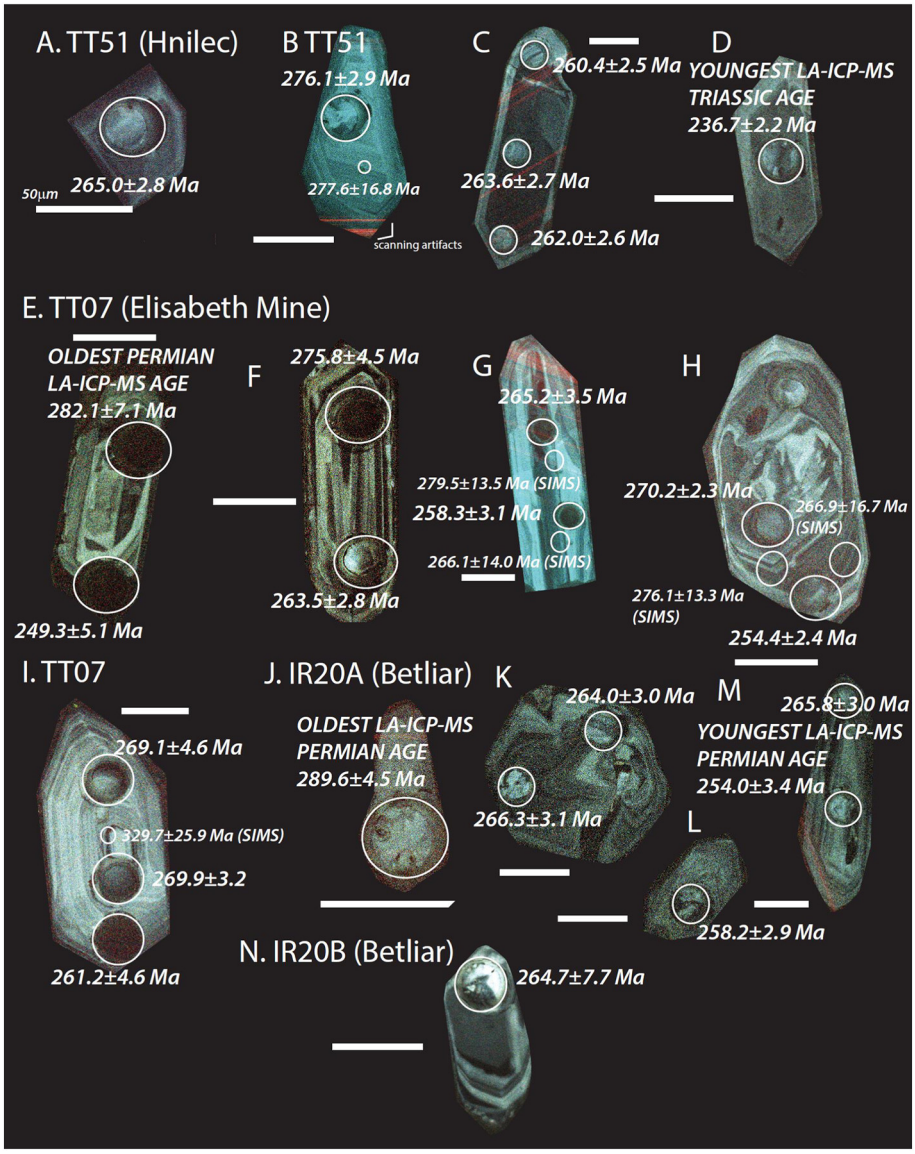

Fig. 7. Color CL images of selected zircons from Hnilec granite sample TT51 (A-D), Elisabeth Mine TT07 (*E*-I), and Beltiar sample IR20A (J-M) and IR20B (panel N). All ages are LA-ICP-MS (± 2σ), except otherwise indicated by a SIMS age (±1σ) in smaller font and with a smaller spot. The dated spots are circled in each panel. Some of the faint red lines seen in some of the zircons are an artifact of the scanning process.

oscillatory zoning in CL, some from sample TT51 and IR20B lack zoning or show recrystallized rims. A correlation between CL color and zircon age could not be detected.

Zircon CL colors in the Hnilec granite are dull blue, purple, green, and yellow, and zircons habits range from equidimensional to prismatic (Fig. 7A–D). Most zircons show oscillatory zoning consistent with magmatic crystallization. Notable exceptions include those with weakly luminescent cores and darker rims and those luminescing in green CL with a complexly zoned core. Despite their zoning differences, these grains yielded ages indifferent from other zircons in the sample. The oldest Permian-age zircon from the Hnilec sample is 286 ± 17 Ma (SIMS). Using LA-ICP-MS, the oldest, more precise Permian age result is 278.7 ± 3.6 Ma. The youngest LA-ICP-MS zircon age from this sample is Triassic (236.7 ± 2.2 Ma) for a zircon core that luminesces a darker blue (Fig. 7D).

Southern Gemeric granite sample TT07 also yields two Triassic LA-ICP-MS zircon U–Pb ages (232.2 ± 4.3 Ma and 249.3 ± 5.1 Ma, Fig. 7E), that are remarkably similar to those of the Hnilec pluton samples. In total, forty-six spots were analyzed on eighteen zircons from sample TT07. The zircons show green and blue colors in CL, and most have distinct cores and show oscillatory zoning, consistent with magmatic crystallization. Some grains exhibit complexly zoned cores (Fig. 7E–I) but yielded ages consistent those obtained from other grains from the same sample. Two zircons yielded two highly imprecise and discordant SIMS Carboniferous ages (306 ± 28 Ma and 330 ± 26 Ma, ±1σ), but such ages are found in the central sections of zircons that yielded Permian results using LA-ICP-MS (e.g., Fig. 7I). The oldest SIMS Permian age is 285 ± 16 Ma (±1σ), which is consistent with the oldest and more precise LA-ICP-MS Permian age of 282.1 ± 7.1 Ma (±2σ) (Fig. 7I). Such ages are also found in the interior of the dated grains. The youngest SIMS age is 261 ± 15 Ma (±1σ).

Two Triassic zircons were also found in Betliar sample IR19B (229.0 ± 3.6 Ma, 241.9 ± 3.4 Ma, LA-ICP-MS). Zircons in Betliar samples IR19A (n = 44 spots) and IR19B (n = 41 spots) were dated using LA-ICP-MS depth-profiling and, therefore, were not imaged in CL. The youngest zircon age from sample IR19A is 252.8 ± 3.2 Ma, which is older than the youngest grains in sample TT51, TT07, and TT48. Two zircons extracted from IR19A and IR19B yield Ordovician, Silurian and Carboniferous ages

(458.4 ± 7.3 Ma and 456.2 ± 7.0 Ma, and 420.3 ± 4.9 Ma and 319 ± 10 Ma, respectively). The oldest Permian grains from samples IR19A and IR19B are similar with ages of 281.2 ± 3.4 Ma and 281.5 ± 3.5 Ma, respectively. Both the average and weighted mean ages that are Permian and younger from these samples are also similar to those from the other Gemeric granite zircons dated in this study (Table 3).

Fig. 7J–N displays the CL images from Betliar samples TT20A and TT20B, which show blue or dark gray luminescence colors. Zircons from sample IR20A are euhedral and subhedral, most showing faint zoning or complexly zoned cores. The zircons were only dated using LA-ICP-MS. Twenty-one spots on 16 grains from sample IR20A yielded Permian ages only, ranging from 289.6 ± 4.5 Ma to 254.0 ± 3.4 Ma (LA-ICP-MS). Sixteen spots on 13 zircons from sample IR20B gave mostly discordant (from 0.6% to 58.2% discordance) with only three showing Permian ages (264.7 ± 7.6 Ma, 275.5 ± 4.4 Ma, and 286.5 ± 4.4 Ma). Most gave Ordovician to Devonian ages and range from 460.3 ± 5.7 Ma to 416.7 ± 7.7 Ma. Most IR20B zircons appear metamict and show no luminescence.

Eleven spots were analyzed on three zircons in Poproč sample TT49. CL zoning of those zircons that showed luminescence consistent with an igneous origin (see Villaseñor et al., 2021 for images). This sample yielded only Permian ages that range from 295.8 ± 3.4 Ma to 261.9 ± 6.5 Ma (LA-ICP-MS). The weighted mean and average ages for the granites are all inconsistent with a single population (Table 3). The oldest Permian weighted mean age (excluding sample IR20B) is from the Poproč granite, (sample TT49, 274.1 ± 1.7 Ma, MSWD = 10.1). The youngest weighted mean U–Pb age stems from the Hnilec pluton (sample TT51, 261.5 ± 0.1 Ma, MSWD = 7).

4.3. Meliata radiolarites

We dated 40 spots on 36 zircon detrital grains extracted from a radiolarite sample (TT08) that overlies altered blueschists in the Meliata Unit (Fig. 8). These detrital zircons range in age from 1522 ± 20 Ma (Mesoproterozoic) to 263.9 ± 2.7 Ma (Permian). Three other Permian zircons overlap in age with the Gemeric granites and Klenovec zircon ages (276.6 ± 5.0 Ma, 288.8 ± 3.9 Ma, and 296.6 ± 3.4 Ma). All of these analyses are concordant. CL images of the grains show green to blue colors, and the youngest zircon has a CL-dark core.

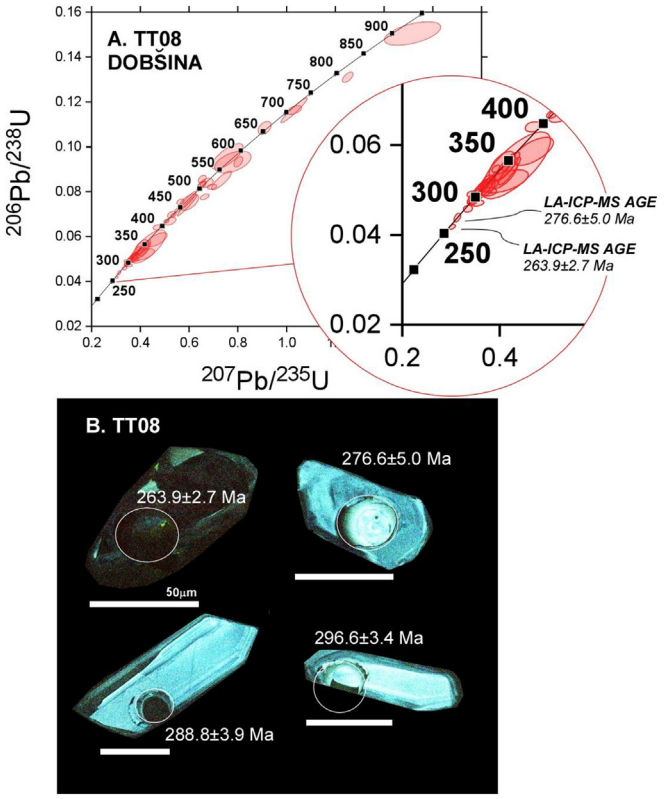

Fig. 8. (A) Concordia diagram of zircons dated from Meliata Unit's radiolarite sample TT08. All ages are LA-ICP-MS (±2σ). (B) CL images of the youngest Permian-age zircons from this sample. The dated spots are circled in each panel.

5. Discussion

The early Paleozoic zircon U–Pb ages from the Gemeric granites dated in this study are Middle Ordovician to Late Silurian (463 ± 11 Ma, 458.4 ± 7.3 Ma, 420.3 ± 4.9 Ma; Table 3, Fig. 6) and are found in the northern Hnilec and southern Betliar granite bodies. These ages are consistent with the widespread occurrence of Ordovician granite associated with arc magmatism along the northern Peri-Gondwanan convergent margin (e.g., Linnemann et al., 2007; von Raumer et al., 2002, 2013; Vozárová et al., 2012). Geochemical data from the Betliar samples indicate that the granites are strongly differentiated, of *syn*-collisional character and must have been generated from a very clay-rich or pelitic source (Fig. 3), consistent with published data for the Gemeric granites (e.g., Broska et al., 2002; Broska and Uher, 2001). The Betliar sample IR20B and Hnilec sample TT51 contain the largest number of inherited early Paleozoic zircons. Geochemical analysis of the IR20B sample indicates it contains the highest Rb, Rb/Ba, FeO/MgO, Sr/Eu contents compared to other Betliar samples (Figs. 2–4). This sample also has Zr/Hf consistent with rare-metal Li–F granites (Fig. 3B) and experienced significant fluid interactions compared to the other Betliar samples (Fig. 4).

A cross-section of the Gemeric Superunit for the Permian (260 Ma, Fig. 9A) illustrates that the granites may have been generated from remnants of (reworked) possible Cambrian basement during post-collisional extension followed by subduction rollback of the Paleo-Tethyan slab in the Permian-Triassic period (Fig. 9B, Froitzheim et al., 2008). Although we did not find evidence for "Pan-African" age (850–550 Ma, see review in Hefferan et al., 2014) in the Gemeric granite zircons dated in this study (Table 3), Ediacaran detrital zircons are common in the Western Carpathian Paleozoic basement (e.g., Kohút et al., 2021; Vozárová et al., 2010, 2012). The specific source of the zircons cannot be conclusively identified by the limited number of zircons dated in this study and a lack of geochemical data from them, but based on the inherited ages and granite geochemical compositions, the source may have accumulated detrital zircons during the Middle Ordovician to Late Silurian. Fig. 9C shows the location of the Gemeric Unit in reference to the Meliata Ocean at 230 Ma.

Most of the zircons from the Gemeric granites dated in the present study yielded Permian-ages, with weighted mean ages of 274.1 ± 1.7 Ma (Poproč) to 261.5 ± 0.1 Ma (Hnilec). The oldest Permian zircons are found in the Betliar (297 ± 15 Ma) and Poproč (295.8 ± 3.4 Ma). In contrast, the youngest zircons are Triassic and are found in the Betliar pluton (229.0 ± 3.6 Ma) and the southern Elisabeth Mine granite (232.6 ± 4.3 Ma). We found no evidence of a southward-decreasing age trend for Gemeric granites, nor any zircon age differences between northern and southern hotline exposures (e.g., Radvanec et al., 2009). Instead, the zircon U–Pb ages demonstrate that the Gemeric granites formed during a single magmatic event and likely share a common source (e.g., Broska and Kubiš, 2019; Broska and Uher, 2001; Kohút, 2012; Petrík and Kohút, 1997; Uher and Broska, 1996). The weighted mean age of zircons dated from the Klenovec granite is likewise Permian (264 ± 0.7 Ma, Table 3), and its youngest zircon is early Triassic (248.6 ± 3.3 Ma). Hence, Permian magmatism was thus not restricted to the Gemeric Superunit and is likewise a characteristic of the Veporic Superunit. The similar intrusion ages of granites in the Gemeric and Veporic units implies that they were likely genetically-related.

Although the dated Gemeric and Veporic Superunit granite samples yielded similar Permian crystallization ages, most Veporic granitoids are Carboniferous in age with Cambrian or Lower to Middle Ordovician

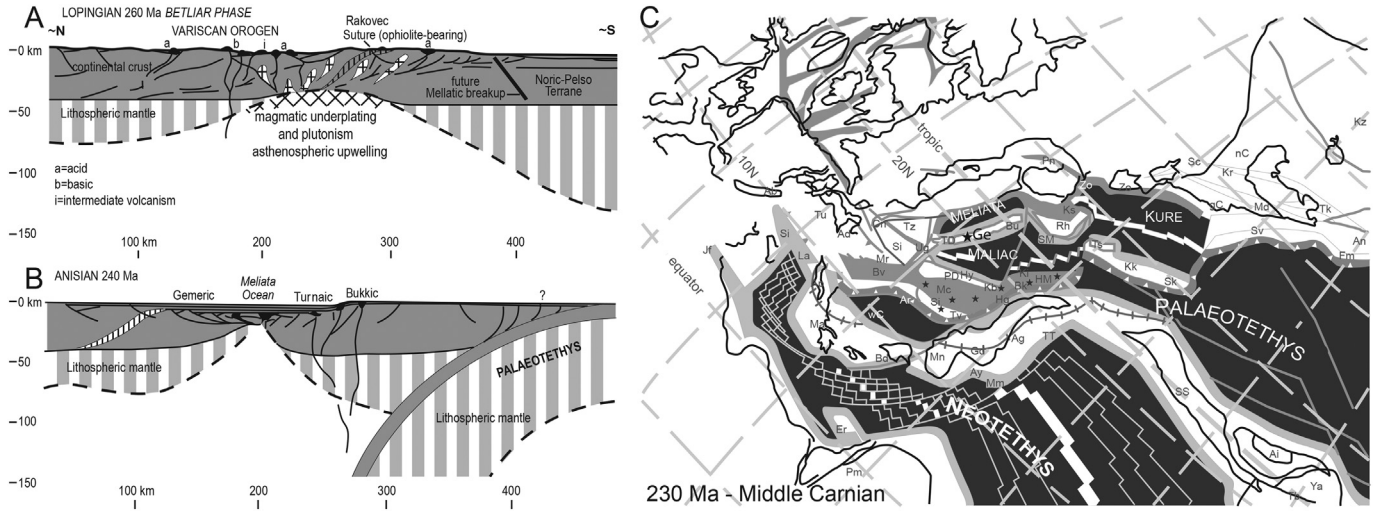

Fig. 9. (A) Paleogeodynamic cross sections across the Western Carpathian orogeny during the Late Permian (260 Ma, Betliar phase) and (B) Anisian (240 Ma, Zarnov phase). Panels and abbreviations after Froitzheim et al. (2008). (C) Paleogeographic reconstruction of the Western Tethys ~230 Ma after Stampfli and Kozur, (2006). See Stampfli and Kozur (2006) for abbreviations. The position of the Gemeric Superunit (Ge) is indicated by a star.

inherited cores (e.g., monazite, 472 ± 4 Ma and 345 ± 3 Ma, Ondrejka e al., 2016; zircon, 514 ± 25 Ma and 348 ± 31 Ma; Putiš et al., 2001; 470–440 Ma and 440–350 Ma, Gaab et al., 2005). Rb–Sr mineral isochrons for Veporic granites are 392 ± 5 Ma and 387 ± 27 Ma (Cambel et al., 1989), whereas discordant zircon ages range from 370 ± 68 Ma and 346 ± 9 Ma (Michalko et al., 1999). Veporic porphyric metadiorites and tonalities gave early Carboniferous zircon ages (357 ± 2 Ma, Broska et al., 2013; 346 ± 1 Ma; Putiš et al., 2001). Similar inherited zircons were documented in this study from the Klenovec (Veporic) and Hnilec (Gemeric) granites. The youngest ages previously reported for the Veporic magmatic assemblages are from early Triassic plagiogranitic-aplite veins that cross-cut basement rocks (zircon U–Pb, 233 ± 4 Ma; Putiš et al., 2001) and a rifting-related biotite leucogranite (Hrončok, zircon thermal ionization mass spectrometry, U–Pb, 238.6 ± 1.4 Ma; Putiš et al., 2000; 267 ± 2 Ma, Ondrejka et al., 2021).

Late to post-Variscan Permian igneous activity has been reported throughout Western Europe (e.g., 285–280 Ma, Ziegler et al., 2004; 295–293 Ma, Timmerman, 2004; 280–240 Ma, McCann et al., 2006; 290–280 Ma). Other granites further east with the Paleo-Tethyan realm record similar ages, such as in Romania (264.2–266.7 Ma, see review in Szemerédi et al., 2020) to the Aegean (e.g., Istanbul-Zonguldak zone's Bolu Massif 273–255 Ma, see review in Ustaömer et al., 2016) and the Cyclades (e.g., Ios Island, Flansburg et al., 2019). The Gemeric and Veporic granites likely were generated during Permian post-collisional extension (e.g., Fig. 9A). This tectono-magmatic scenario is characteristic for the Permian of the Central and Southern Alps, Western Carpathians, and Western Mediterranean (e.g., Broska and Kubiš, 2019; Putiš et al., 2000; Ustaömer et al., 2016). The widespread occurrence of Permian magmatism in the European Variscan domain has been interpreted as evidence for regional magmatic destabilization of the Moho in response to a thermal surge (Fig. 9A) (e.g., Ziegler et al., 2004). The surge involved significant lower crustal melting, upward displacement of the Moho, and delamination of the mantle-lithosphere, which contributed substantially towards the thinning of the Variscan crust (e.g., Froitzheim et al., 2008).

The Veporic zircons differ from the Gemeric zircons in that they have distinct yellow rims in CL (Fig. 6), a feature not observed in the Gemeric zircons. The yellow CL color is characteristic of lower temperatures compared to blue luminescence (e.g., Tsuchiya et al., 2015). Although the narrowness and location of the rims precluded dating in spot mode on exposed cross sections, we suspect they are likely to be due to subsequent Alpine alteration or re-heating that affected the Veporic Superunit, and that this did not occur in the Gemeric samples. The zircon saturation temperatures for both Gemeric and Veporic granites are similar (Table 2), so the presence of the lower temperature overprints was likely caused by Alpine deformation events. The Veporic Superunit also experienced by Cretaceous magmatism (e.g., 75.6 ± 1.1 Ma, Poller et al., 2001; 82 ± 1 Ma, Hraško et al., 1999; 81.5 ± 0.7 Ma, Kohút et al., 2013).

Fig. 10 shows a probability density diagram for zircon U–Pb ages from the granites of the Gemeric Superunit, the Veporic Superunit's Klenovec granite (TT48), and the Meliata Unit's radiolarite (TT08). All plots show identical major mid-Permian age maxima for the Veporic granite (265.2 Ma), Gemeric granites (264.3 Ma), and Meliata radiolarite (264.0 Ma). The detrital zircon ages obtained for the Meliata radiolarite reveal distinct peaks in the age probability distribution that are nearly identical to the Veporic and Gemeric granites. Most of the Permian detrital zircons also show blue colors in CL and oscillatory zoning, consistent with a volcanic origin. Permian volcanic rocks have long

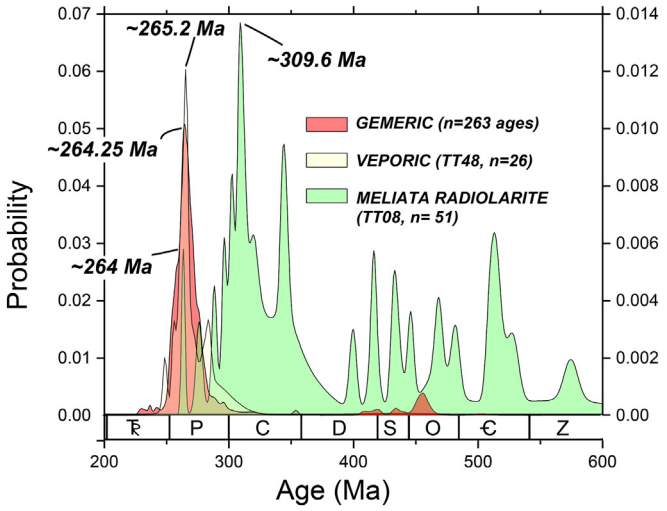

Fig. 10. Probability density diagram of zircons ages from the Gemeric and Veporic superunits and the Meliata Unit's radiolarite dated in this study. The peaks of the Permian ages from these samples are indicated. The right y-axis is relevant to the Meliata Unit's zircon ages, whereas the left y-axis is for the Gemeric and Veporic superunit granite zircon ages.

been recognized in different parts of the Carpathian–Pannonian region (e.g., Dostal et al., 2003; Vozárová et al., 2012; Szemerédi et al., 2020). Hence, numerous options exist for volcanic terranes in the vicinity of the Meliata Ocean that could have provided Permian igneous zircons similar to those dated in the radiolarites.

The age probability density diagram (Fig. 10) for the Meliata Unit shows that the youngest zircon dated in the sample is 263.9 ± 2.7 Ma. Based on previous published work, structural relationships, fossil contents, and proximity, we propose that the radiolarite unit was deposited in the Meliata Ocean (e.g., Putiš et al., 2019) and is characterized by a ~ 264 maximum depositional age for the Dobšiná location at that time. This age is consistent with the timing of opening of the Meliata Ocean due to the northwestern subduction of the Paleotethyan Ocean (e.g., Putiš et al., 2019). Radiolarians in carbonate strata that overlie the blueschist and harzburgite-lizardite serpentinite assemblages south of Dobšiná indicate Jurassic deposition in distal flysch (Havrila and Ožvoldová, 1996). Fig. 9C shows a paleogeographic reconstruction of the region with the Meliata Ocean clearly developed by 230 Ma (Stampfli and Kozur, 2006). This is consistent with our zircon ages indicating that Meliata Ocean pelagic sedimentation likely initiated during the mid-Permian (~264 Ma).

The most abundant detrital zircon age peak in the probability density diagram for sample TT08 is Carboniferous (~310 Ma; Fig. 10), which correlates well with the ages of ignimbrites associated with large volcanic centers that developed within the Variscan realm, such as the Teplice-Altenberg Volcanic Center (Erzgebirge, Germany) or the Brandov-Olbernhau Basin (see Hoffmann et al., 2013; Opluštil et al., 2016).

6. Conclusions

The age and composition of the granites within and surrounding the Gemeric Superunit are critical for understanding and constraining the evolution of the present Western Carpathian Mountains and deciphering its relationship to other tectonic units in central and eastern Europe exposed along the Paleotethyan Ocean (e.g., Broska and Kubiš, 2019; Froitzheim et al., 2008; Lexa et al., 2003). The Gemeric Superunit (Western Carpathians) is characterized by Permian rare-metal granites that formed from pelitic sources, likely due to post-orogenic extension of crust thickened after the collisional phase of the Variscan orogeny. Based on the inherited zircon ages and Gemeric granite geochemical compositions, the source may have accumulated detrital zircons during the Middle Ordovician to Late Silurian. The Gemeric Superunit correlates with lower structural levels of the Austroalpine nappe system. Zircon ages from northern (Hnilec) and southern Gemeric granites (Betliar, Elisabeth Mine, Poproč) yielded Permian zircon U–Pb ages that overlap with those of the Klenovec granite found in the adjacent Veporic Superunit. Color CL images of the Klenovec zircons show yellow luminescence, consistent with lower temperature and likely the result of an intensive Alpine-related imprint not found in the Gemeric zircons. The zircon ages, however, indicate similar sources and provide further evidence of widespread Permian magmatism that extends from the European Variscan internal domain to the western Mediterranean. The ages of the Gemeric and Veporic granites also overlap the youngest zircons from sediments that overlie parts of the Meliata Ocean units. Although the detrital zircons in the Meliata radiolarite may have been sourced from multiple volcanic centers active throughout the region, sedimentation in this ocean fragment may have begun during the mid-Permian (~264 Ma).

Declaration of Competing Interest

The authors declare that they have no known competing financial interests or personal relationships that could have appeared to influence the work reported in this paper.

Acknowledgements

This work was supported by the National Science Foundation (NSF), grant number 1460050. IB and MK were supported by the Slovak Research and Development Agency, grant number APVV-18-0107 and VEGA 2/0075/20. We appreciate support from UT Austin's Center for Russian, East European, and Eurasian Studies (CREEES) and Undergraduate Research Fellowship (URF) programs. We appreciate field assistance and discussions with Brent A. Elliott, Thomas Quintero, Theresa Perez, Saloni Tandon, and Zoe Yin. We appreciate analytical assistance from Beth-Anne Belle at the UCLA SIMS facility and Lisa Stockli at the UT Austin (U–Th)/He and U–Pb Geo-Thermochronometry Lab. The ion microprobe facility at UCLA is partly supported by a grant from the Instrumentation and Facilities Program, Division of Earth Sciences, NSF. We appreciate drafting assistance from Jeffrey Horowitz (Dept. Geological Sciences, Jackson School, UT Austin) and analytical assistance on the FEI Nova Nano SEM from Priyanka Periwal (Bureau of Economic Geology, Jackson School, UT Austin). Comments from three anonymous reviewers improved the original manuscript.

References

Árkai, P., Faryad, S.W., Vidal, O., Balogh, K., 2003. Very low-grade metamorphism of sedimentary rocks of the Meliata unit, Western Carpathians, Slovakia: implications of phyllosilicate characteristics. Int. J. Earth Sci. (Geol. Rundsch.) 92, 68–85. https://doi.org/10.1007/s00531-002-0303-x.

Bajaník, S., Hanzel, V., Ivanička, J., Mello, J., Pristaš, J., Reichwalder, P., Snopko, L., Vozár, J., Vozárová, A., 1983. Explanations to the Geological Map of the Slovak Ore Mountains 1:50 000. Dionýz Štúr Institute of Geology, Bratislava, pp. 1–224 (In Slovak with English summary).

Breiter, K., Broska, I., Uher, P., 2015. Intensive low-temperature tectono-hydrothermal overprint of peraluminous rare-metal granite; a case study from the Dlha Dolina Valley (Gemericum, Slovakia). Geol. Carpathica (Bratislava) 66, 19–36.

Broska, I., Kubiš, M., 2018. Accessory minerals and evolution of tin-bearing S-type granites in the Western segment of the Gemeric Unit (Western Carpathians). Geol. Carpath. 69, 483–497.

Broska, I., Kubiš, M., 2019. Whole rock chemistry of the Permian Gemeric specialized S-type granites (Western Carpathians) and remark to their correlation. Geol. Carpathica (Bratislava) 70, 112–114.

Broska, I., Uher, P., 2001. Whole-rock chemistry and genetic typology of the West-Carpathian Variscan granites. Geol. Carpathica (Bratislava) 52, 79–90.

Broska, I., Kubiš, M., Williams, C.T., Konečný, P., 2002. The compositions of rock-forming and accessory minerals from the Gemeric granites (Hnilec area, Gemeric superunit, Western Carpathians). In: Breiter, K. (Ed.), Selected Papers Presented on International Workshop "Phosphorus- and Fluorine-Rich Fractionated Granites," Vestnik Ceskeho Geologickeho Ustavu = Bulletin of the Czech Geological Survey. 77, pp. 147–155.

Broska, I., Petrík, I., Be'eri-Shlevin, Y., Majka, J., Bezák, V., 2013. Devonian/Mississippian I-type granitoids in the Western Carpathians: A subduction-related hybrid magmatism. Lithos 162–163, 27–36.

Cambel, B., Bagdasaryan, G.P., Gukasyan, R.C., Veselsky, J., 1989. Rb-Sr geochronology of leucocratic granitoid rocks from the Spissko-gemerske rudohorie Mts. And Veporicum. Geol. Zbor. Geol. Carpathica (Bratislava) 40, 323–332.

Channell, J.E.T., Kozur, H.W., 1997. How many oceans? Meliata, Vardar and Pindos oceans in Mesozoic Alpine paleogeography. Geology (Boulder) 25, 183–186.

Dallmeyer, R.D., Neubauer, F., Handler, R., Fritz, H., Muller, W., Pana, D., Putiš, M., 1996. Tectonothermal evolution of the internal Alps and Carpathians: 40Ar/39Ar mineral and whole rock data. Eclogae Geol. Helv. 89, 203–277.

Dallmeyer, R.D., Neubauer, F., Fritz, H., 2008. The Meliata Suture in the Carpathians; regional significance and implications for the evolution of high-pressure wedges within collisional orogens. In: Siegesmund, S., Fuegenschuh, B., Froitzheim, N. (Eds.), Tectonic Aspects of the Alpine-Dinaride-Carpathian System. Geological Society Special Publications vol. 298, pp. 101–115.

Dehaine, Q., Filippov, L.O., Glass, H.J., Rollinson, G., 2019. Rare-metal granites as a potential source of critical metals: A geometallurgical case study. Ore Geol. Rev. 104, 384–402. https://doi.org/10.1016/j.oregeorev.2018.11.012.

Dostal, J., Vozár, J., Keppie, J.D., Hovorka, D., 2003. Permian volcanism in the Central Western Carpathians (Slovakia): Basin-and-Range type rifting in the southern Laurussian margin. Int. J. Earth Sci. (Geol. Rundsch.) 92, 27–35. https://doi.org/10.1007/s00531-002-0307-6.

Faryad, S.W., Henjes-Kunst, F., 1997. Petrological and K-Ar and ^{40}Ar-^{39}Ar age constraints for the tectonothermal evolution of the high-pressure Meliata unit, Western Carpathians (Slovakia). Tectonophysics 280, 141–156. https://doi.org/10.1016/S0040-1951(97)00141-8.

Faryad, S.W., Spišiak, J., Horvath, P., Hovorka, D., Dianiška, I., Jozsa, S., 2005. Petrological and geochemical features of the Meliata mafic rocks from the sutured Triassic oceanic basin, Western Carpathians. Ofioliti 30, 27–35.

Faryad, S.W., Ivan, P., Jedlička, R., 2020. Pre-Alpine high-pressure metamorphism in the Gemer unit: mineral textures and their geodynamic implications for Variscan Orogeny in the Western Carpathians. Int. J. Earth Sci. 109, 1547–1564. https://doi.org/10.1007/s00531-020-01856-2.

Finger, F., Broska, I., 1999. The Gemeric S-type granites in southeastern Slovakia: late Palaeozoic or Alpine intrusion? Evidence from the electron-microprobe dating of monazite. Schweizerische Mineralogische und Petrographische Mitteilungen = Swiss Bulletin of. Mineral. Petrol. 79, 439–443.

Flansburg, M.E., Stockli, D.F., Poulaki, E.M., Soukis, K., 2019. Tectono-magmatic and stratigraphic evolution of the Cycladic Basement, Ios Island, Greece. Tectonics 38, 2291–2316. https://doi.org/10.1029/2018TC005436.

Froitzheim, N., Plašienka, D., Schuster, R., 2008. Alpine tectonics of the Alps and Western Carpathians. In: McCann, T. (Ed.), The Geology of Central Europe. Vol. 2. https://doi.org/10.1144/CEV2P.6 Mesozoic and Cenozoic.

Frost, B.R., Barnes, C.G., Collins, W.J., Arculus, R.J., Ellis, D.J., Frost, C.D., 2001. A Geochemical Classification for Granitic Rocks. J. Petrol. 42, 2033–2048. https://doi.org/10.1093/petrology/42.11.2033.

Gaab, A.S., Poller, U., Janak, M., Kohút, M., Todt, W., 2005. Zircon U-Pb geochronology and isotopic characterization for the pre-Mesozoic basement of the northern Veporic Unit (central Western Carpathians, Slovakia). Schweizerische Mineralogische und Petrographische Mitteilungen = Bulletin Suisse de Mineralogie et Petrographie 85, 69–88.

Gao, S., Luo, T.-C., Zhang, B.-R., Zhang, H.-F., Han, Y.-w., Zhao, Z.-D., Yi-Ken Hu, Y.-K., 1998. Chemical composition of the continental crust as revealed by studies in East China. Geochim. Cosmochim. Acta 62, 1959–1975. https://doi.org/10.1016/S0016-7037(98)00121-5.

Grecula, P., Abonyi, A., Abonyiova, M., Antas, J., Bartalsky, B., Bartalsky, J., et al., 1995. Mineral Deposits of the Slovak Ore Mountains. Mineralia Slovaca – Monograph, Bratislava.

Havrila, M., Ožvoldová, L., 1996. Meliaticum in the Stratenska hornatina Hills. Slovak Geol. Mag. 3-4 (96), 335–339.

Hefferan, K., Soulaimani, A., Samson, S.D., Admou, H., Inglis, J., Saquaque, A., Latifa, C., Heywood, N., 2014. A reconsideration of Pan African orogenic cycle in the Anti-Atlas Mountains, Morocco. J. Afr. Earth Sci. 98, 34–46. https://doi.org/10.1016/j.jafrearsci.2014.03.007.

Hoffmann, U., Breitkreuz, C., Breiter, K., Sergeev, S., Stanek, K., Tichomirowa, M., 2013. Carboniferous–Permian volcanic evolution in Central Europe—U/Pb ages of volcanic rocks in Saxony (Germany) and northern Bohemia (Czech Republic). Int. J. Earth Sci. 102, 73–99. https://doi.org/10.1007/s00531-012-0791-2.

Horbe, M.A., Horbe, A.C., Costi, H.T., Teixeira, J.T., 1991. Geochemical characteristics of cryolite-tin-bearing granites from the Pitinga Mine, northwestern Brazil — A review. J. Geochem. Explor. 40, 227–249. https://doi.org/10.1016/0375-6742(91)90040-2.

Hraško, Ľ., Határ, J., Michalko, J., Huhma, H., Mäntäri, I., Vaasjoki, M., 1999. U/Pb zircon dating of the Upper cretaceous granite (Rochovce type) in Western Carpathians. Krystalinikum, (Brno). 25, pp. 163–171.

Hraško, L., Broska, I., Finger, F., 2002. Permian granitic magmatism and disintegration of the Lower Paleozoic basement in the SW veporicum near Klenovec (Western Carpathians). In: Michalik, J., Šimon, L., Vozár, J. (Eds.), Proceedings of XVII. Congress of Carpathian–Balkan Geological Association Bratislava, September 1st–4th. 53, p. 7.

Hrouda, F., Faryad, S.W., 2017. Magnetic fabric overprints in multi-deformed polymetamorphic rocks of the Gemeric Unit (Western Carpathians) and its tectonic implications. Tectonophysics 717, 83–98.

Hurai, V., Lexa, O., Schulmann, K., Montigny, R., Prochaska, W., Frank, W., Konečný, P., Král, J., Thomas, R., Chovan, M., 2008. Mobilization of ore fluids during Alpine metamorphism: evidence from hydrothermal veins in the Variscan basement of Western Carpathians, Slovakia. Geofluids 8, 181–207. https://doi.org/10.1111/j.1468-8123.2008.00216.x.

Hurai, V., Chovan, M., Huraiová, M., Koděra, P., Konečný, P., Lexa, O., 2010. Slovak Ore Mountains: Origin of hydrothermal mineralization and environmental impacts of mining. Acta Mineral. Petrograph. 28, 1–36.

Irber, W., 1999. The lanthanide tetrad effect and its correlation with K/Rb, Eu/Eu*, Sr/Eu, Y/Ho, and Zr/Hf of evolving peraluminous granite suites. Geochim. Cosmochim. Acta 63, 489–508. https://doi.org/10.1016/S0016-7037(99)00027-7.

Jakabská, K., Rozložník, L., 1989. Zircons of Gemeric granites (West Carpathians, Czechoslovakia). Geol. Carpathica (Bratislava) 40, 141–160.

Jeřábek, P., Janák, M., Faryad, S.W., Finger, F., Konečný, P., 2008. Polymetamorphic evolution of pelitic schists and evidence for Permian low-pressure metamorphism in the Vepor Unit, West Carpathians. J. Metamorph. Geol. 26, 465–485. https://doi.org/10.1111/j.1525-1314.2008.00771.x.

Kohút, M., 2012. Genesis of the Germeric granites in the light of isotope geochemistry: Separated facts from myth. Min. Slovaca 44, 89.

Kohút, M., Stein, H., 2005. Re–Os molybdenite dating of granite-related Sn–W–Mo mineralisation at Hnilec, Gemeric Superunit, Slovakia. Mineral. Petrol. 85, 117–129. https://doi.org/10.1007/s00710-005-0082-8.

Kohút, M., Stein, H., Uher, P., Zimmerman, A., Hrasko, L., 2013. Re-Os and U-Th-Pb dating of the Rochovce Granite and its mineralization (Western Carpathians, Slovakia). Geol. Carpathica (Bratislava) 64, 71–79. https://doi.org/10.2478/geoca-2013-0005.

Kohút, M., Linnemann, U., Hofmann, M., Gärtner, A., Zieger, J., 2021. Provenance and detrital zircon study of the Western Carpathians basement. In: Linnemann, U. (Ed.), Geology of the Central European Variscides and its Avalonian–Cadomian precursors. Springer Monograph.

Kovách, Á., Svingor, E., Grecula, P., 1986. Rb/Sr isotopic ages of granitoide rocks from the Spišsko–gemerske rudohorié Mts., West Carpathians, Eastern Slovakia. Mineralia Slovaca 18, 1–14.

Kozur, H., Mock, R., 1997. New paleogeographic and tectonic interpretations in the Slovakian Carpathians and their implications for correlations with the Eastern Alps and other parts of the Western Tethys. Part II: Inner Western Carpathians. Mineralia Slovaca 3 (1997), 164–209.

Kubiš, M., Broska, I., 2005. The role of boron and fluorine in evolved granite rock systems (on the example of the Hnilec area, Western Carpathians). Geol. Carpathica (Bratislava) 56, 193–204.

Kubiš, M., Broska, I., 2010. The granite system near Betliar village (Gemeric Superunit, Western Carpathians): evolution of a composite silicic reservoir. J. Geosci. 55, 131–148.

Lexa, J., Bezák, V., Elečko, M., Eliáš, M., Konečný, V., Less, G.Y., Mandl, W., Mello, J., Pálenský, P., Pelikán, P., Polák, M., Potfaj, M., Radocz, G.Y., Rylko, W., Schnabel, G.W., Stránik, Z., Vass, D., Vozár, J., Zelenka, T., Biely, A., Császár, G., Čtyroký, P., Kaličiak, M., Kohút, M., Kovacs, S., Mackiv, B., Maglay, J., Nemčok, J., Nowotný, A., Pentelényi, L., Rakús, M., Vozárová, A., 2000. Geological map of Western Carpathians and Adjacent Areas 1 : 500 000. Dionýz Štúr Publishing House, Bratislava.

Lexa, O., Schulmann, K., Ježek, J., 2003. Cretaceous collision and indentation in the West Carpathians: View based on structural analysis and numerical modeling. Tectonics, 22 https://doi.org/10.1029/2002TC001472.

Linnemann, U., Gerdes, A., Drost, K., Buschmann, B., 2007. The continuum between Cadomian orogenesis and opening of the Rheic Ocean: Constraints from LA-ICP-MS U-Pb zircon dating and analysis of plate-tectonic setting (Saxo-Thuringian zone, northeastern Bohemian Massif, Germany). Special Papers-Geol. Soc. Am. 423, 61–96. https://doi.org/10.1130/2007.2423(03).

Maluski, H., Rajlich, P., Matte, P., 1993. ^{40}Ar-^{39}Ar dating of the Inner Carpathians Variscan basement and Alpine mylonitic overprinting. Tectonophysics 223, 313–337.

McCann, T., Pascal, C., Timmerman, M.J., Krzywiec, P., López-Gómez, J., Wetzel, L., Krawczyk, C.M., Rieke, H., Lamarche, J., 2006. Post-Variscan (end Carboniferous-early Permian) basin evolution in Western and Central Europe. Geol. Soc. Lond. Mem. 32, 355–388. https://doi.org/10.1144/GSL.MEM.2006.032.01.22.

Michalko, J., Bezák, V., Král, J., Huhma, H., Mäntäri, I., Vaasjoki, M., Broska, I., Hraško, L., Határ, J., 1999. U/Pb zircon data from the Veporic granitoids (Western Carpathians). Krystalinikum 24, 91–104.

Mock, R., Sykora, M., Aubrecht, R., Ozvoldova, L., Kronome, B., Reichwalder, P., Jablonsky, J., 1998. Petrology and stratigraphy of the Meliaticum near the Meliata and Jaklovce villages, Slovakia. Slovak Geol. Mag. 4, 223–260.

Monecke, T., Kempe, U., Monecke, J., Sala, M., Wolf, D., 2002. Tetrad effect in rare earth element distribution patterns: a method of quantification with application to rock and mineral samples from granite-related rare metal deposits. Geochim. Cosmochim. Acta 66, 1185–1196. https://doi.org/10.1016/S0016-7037(01)00849-3.

Ondrejka, M., Uher, P., Putiš, M., Kohút, M., Broska, I., Larionov, A., Bojar, A.-V., Sobocký, T., 2021. Permian A-type granites of the Western Carpathians and Pannonian region: products of the Pangea break-up. Int. J. Earth Sci. IJES-D-020-00459, in review.

Opluštil, S., Schmitz, M., Kachlík, V., Štamberg, S., 2016. Re-assessment of lithostratigraphy, biostratigraphy, and volcanic activity of the late Paleozoic Intra-Sudetic, Krkonoše-Piedmont and Mnichovo Hradiště basins (Czech Republic) based on new U-Pb CA-ID-TIMS ages. Bull. Geosci. 91, 399–432. https://doi.org/10.3140/bull.geosci.1603.

Patino Douce, A.E., 1999. What do experiments tell us about relative contributions of crust and mantle to the origin of granitic magmas? Geol. Soc. Spec. Publ. 168, 55–75. https://doi.org/10.1144/GSL.SP.1999.168.01.0516855-75.

Pearce, J.A., Harris, N.B.W., Tindle, A.G., 1984. Trace element discrimination diagrams for the tectonic interpretation of granitic rocks. J. Petrol. 25, 956–983. https://doi.org/10.1093/petrology/25.4.956.

Petrasová, K., Faryad, S.W., Jeřábek, P., Žáčková, E., 2007. Origin and metamorphic evolution of magnesite-talc adjacent rocks near Gemerská Poloma, Slovak Republic. J. Geosci. 52, 125–132.

Petrík, L., Kohút, M., 1997. The evolution of granitoid magmatism during the Variscan orogen in the Western Carpathians. In: Grecula, P., Hovorka, D., Putiš, M. (Eds.), Geological Evolution of the Western Carpathians. Mineralia Slovaca. Monographs, Bratislava, pp. 235–252.

Petrík, I., Kubiš, M., Konečný, P., Broska, I., Malachovský, P., 2011. Rare phosphates from the Surovec topaz-Li-mica microgranite, Gemeric unit, Western Carpathians, Slovakia: the role of the F/H2O in the melt. Can. Mineral. 49, 521–540.

Petrík, I., Čík, Š., Miglierini, M., Vaculovič, T., Dianiška, I., Ozdín, D., 2014. Alpine oxidation of lithium micas in Permian S-type granites (Gemeric unit, Western Carpathians, Slovakia). Mineral. Mag. 78, 507–533. https://doi.org/10.1180/minmag.2014.078.3.03.

Plašienka, D., Méres, Š., Ivan, P., Sýkora, M., Soták, J., Lačný, A., Aubrecht, R., Bellová, S., Potočný, T., 2019. Meliatic blueschists and their detritus in cretaceous sediments: new data constraining tectonic evolution of the West Carpathians. Swiss J. Geosci. 112, 55–81. https://doi.org/10.1007/s00015-018-0330-7.

Poller, U., Uher, P., Janák, M., Plašienka, D., Kohút, M., 2001. Late cretaceous age of the Rochovce Granite, Western Carpathians, constrained by U-Pb single-zircon dating in combination with cathodoluminescence imaging. Geol. Carpathica (Bratislava) 52, 41–47.

Poller, U., Uher, P., Broska, I., Plašienka, D., Janák, M., 2002. First Permian-early Triassic zircon ages for tin-bearing granites from the Gemeric Unit (Western Carpathians, Slovakia); connection to the post-collisional extension of the Variscan Orogen and S-type granite magmatism. Terra Nova 14, 41–48.

Putiš, M., Kotov, A.B., Uher, P., Salnikova, E.B., Korikovsky, S.P., 2000. Triassic age of the Hroncok pre-orogenic A-type granite related to continental rifting; a new results of U-Pb isotope dating (Western Carpathians). Geol. Carpathica (Bratislava) 51, 59–66.

Putiš, M., Kotov, A.B., Korikovsky, S.P., Salnikova, E.B., Yakovleva, S.Z., Berezhnaya, N.G., Kovach, V.P., Plotkina, J.V., 2001. U-Pb zircon ages of dioritic and trondhjemitic rocks from a layered amphibolitic complex cross-cut by granite vein (Veporic Basement, Western Carpathians). Geol. Carpathica (Bratislava) 52, 49–60.

Putiš, M., Koppa, M., Snarska, B., Koller, F., Uher, P., 2012. The blueschist-associated perovskite-andradite-bearing serpentinized harzburgite from Dobšiná (the Meliata Unit), Slovakia. J. Geosci. 57, 221–240.

Putiš, M., Koller, F., Li, X.-H., Qui-Li, L., Larionov, A., Siman, P., Ondrejka, M., Uher, P., Németh, Z., Ružička, P., Nemec, O., 2019. Geochronology of Permian–Triassic tectono–magmatic events from the Inner Western Carpathian and Austroalpine units. Geol. Carpath. 70 Smolenice, October 9–11.

Radvanec, M., Koděra, P., Prochaska, W., 2004. Mg replacement at the Gemerská Poloma talc-magnesite deposit, Western Carpathians, Slovakia. Acta Petrol. Sin. 20, 773–790.

Radvanec, M., Konečný, P., Ondrejka, M., Putiš, M., Uher, P., Németh, Z., 2009. The Gemeric granites as an indicator of the crustal extension above the Late-Variscan subduction zone and during the early Alpine riftogenesis (Western Carpathians): an interpretation from the monazite and zircon ages dated by CHIME and SHRIMP methods. Min. Slovaca 41, 381–394.

Schmid, S.M., Bernoulli, D., Fügenschuh, B., Matenco, L., Schefer, S., Schuster, R., Tischler, M., Ustaszewski, K., 2008. The Alpine-Carpathian-Dinaridic orogenic system: correlation and evolution of tectonic units. Swiss J. Geosci. 101, 139–183. https://doi.org/10.1007/s00015-008-1247-3.

Šefara, J., Bielik, M., Vozár, J., Katona, M., Szalaiová, V., Vozárová, A., Šimonová, B., Pánisová, J., Schmidt, S., Götze, H.-J., 2017. 3D density modelling of Gemeric granites of the Western Carpathians. Geol. Carpathica (Bratislava) 68, 177–192. https://doi.org/10.1515/geoca-2017-0014.

Stampfli, G.M., Kozur, H.W., 2006. Europe from the Variscan to the Alpine cycles. In: Gee, D.G., Stephenson, R.A. (Eds.), European Lithosphere Dynamics. Memoirs of the Geological Society of London vol. 32, pp. 57–82.

Sun, S.S., McDonough, W.F., 1989. Chemical and isotopic systematics of oceanic basalts: Implications for mantle composition and processes. Geol. Soc. Lond., Spec. Publ. 42, 313–345. https://doi.org/10.1144/GSL.SP.1989.042.01.19.

Sylvester, P.J., 1998. Post-collisional strongly peraluminous granites. Lithos 45, 29–44. https://doi.org/10.1016/S0024-4937(98)00024-3.

Szemerédi, M., Lukács, R., Varga, A., Dunkl, I., Józsa, S., Tatu, M., Pál-Molnár, E., Szepesi, J., Guillong, M., Szakmány, G., Harangi, S., 2020. Permian felsic volcanic rocks in the Pannonian Basin (Hungary): new petrographic, geochemical, and geochronological results. Int. J. Earth Sci. 109, 101–125. https://doi.org/10.1007/s00531-019-01791-x.

Taylor, S.R., McLennan, S.M., 1985. The Continental Crust: Its Composition and Evolution. Blackwell, Oxford Press, p. 312.

Timmerman, M.J., 2004. Timing, geodynamic setting and character of Permo-Carboniferous magmatism in the foreland of the Variscan Orogen, NW Europe. Geol. Soc. Lond., Spec. Publ. 223, 41–74. https://doi.org/10.1144/GSL.SP.2004.223.01.03a.

Tsuchiya, Y., Kayama, M., Nishida, H., Noumi, Y., 2015. Annealing effects on cathodoluminescence of zircon. J. Mineral. Petrol. Sci. 110, 283–292.

Uher, P., Broska, I., 1996. Post-orogenic Permian granitic rocks in the Western Carpathian-Pannonian area: Geochemistry, mineralogy and evolution. Geol. Carpathica (Bratislava) 47, 311–321.

Ustaömer, T., Ustaömer, P.A., Robertson, A.H.F., Gerdes, A., 2016. Implications of U–Pb and Lu–Hf isotopic analysis of detrital zircons for the depositional age, provenance and tectonic setting of the Permian–Triassic Palaeotethyan Karakaya complex, NW Turkey. Int. J. Earth Sci. 105, 7–38. https://doi.org/10.1007/s00531-015-1225-8.

Villaseñor, G., Catlos, E.J., Broska, I., Kohút, M., Hraško, L., Aguilera, K., Etzel, T.M., Kyle, J.R., Stockli, D.F., 2021. Western Carpathian mid-Permian Magmatism: Petrographic, Geochemical, and Geochronological Data. Data in Brief In press.

von Raumer, J.F., Stampfli, G.M., Borel, G.D., Bussy, F., 2002. Organization of pre-Variscan basement areas at the north-Gondwanan margin. Int. J. Earth Sci. 91, 35–52. https://doi.org/10.1007/s005310100200.

von Raumer, J.F., Bussy, F., Schaltegger, U., Schulz, B., Stampfli, G.M., 2013. Pre-Mesozoic Alpine basements—their place in the European Paleozoic framework. GSA Bull. 125, 89–108. https://doi.org/10.1130/B30654.1.

Vozárová, A., Šarinová, K., Larionov, A., Presnyakov, S., Sergeev, S., 2010. Late Cambrian/Ordovician magmatic arc type volcanism in the Southern Gemericum basement, Western Carpathians, Slovakia: U-Pb (SHRIMP) data from zircons. Int. J. Earth Sci. 99, S17–S37.

Vozárová, A., Šarinová, K., Rodionov, N., Laurinc, D., Paderin, I., Sergeev, S., Lepkhina, E., 2012. U-Pb ages of detrital zircons from Paleozoic metasandstones of the Gelnica terrane (Southern Gemeric unit, Western Carpathians, Slovakia): evidence for Avalonian Amazonian provenance. Int. J. Earth Sci. 101, 919–936. https://doi.org/10.1007/s00531-011-0705-8.

Whalen, J.B., Currie, K.L., Chappell, B.W., 1987. A-type granites: Geochemical characteristics, discrimination and petrogenesis. Contrib. Mineral. Petrol. 95, 407–419.

Zaraisky, G.P., Aksyuk, A.M., Devyatova, V.N., Udoratina, O.V., Chevychelov, V.Y., 2008. Zr/Hf ratio as an indicator of fractionation of rare-metal granites by the example of the Kukulbei complex, eastern Transbaikalia. Petrology 17, 25–45. https://doi.org/10.1134/S0869591108070047.

Zhenhua, Z., Masuda, A., Shabani, M.B., 1993. REE tetrad effects in rare-metal granites. Chin. J. Geochem. 12, 206–219. https://doi.org/10.1007/BF02843360.

Ziegler, P.A., Schumacher, M.E., Dèzes, P., Van Wees, J.-D., Cloetingh, S., 2004. Post-Variscan evolution of the lithosphere in the Rhine Graben area: constraints from subsidence modelling. Geol. Soc. Lond., Spec. Publ. 223, 289–317. https://doi.org/10.1144/GSL.SP.2004.223.01.13.